August 2020

Investigation of Co-Pyrolysis and Co-Gasification of Chicken Manure and Rice Husk

Juan Camilo Espindola Canon
University of Wisconsin-Milwaukee

INVESTIGATION OF CO-PYROLYSIS AND CO-GASIFICATION OF CHICKEN MANURE AND RICE HUSK

by

Juan C Espindola

A Thesis Submitted in

Partial Fulfillment of the

Requirements for the degree of

Master of Science

in Engineering

at

The University of Wisconsin-Milwaukee

August 2020

ABSTRACT

INVESTIGATION OF CO-PYROLYSIS AND CO-GASIFICATION
OF CHICKEN MANURE AND RICE HUSK

by

Juan Espindola

The University of Wisconsin-Milwaukee,2020
Under the supervision of Professor Ryoichi Amano

Renewable energy is gaining more attention to supply the increasing energy demand worldwide. Currently, biomass is gaining popularity because this energy source offers several flexibilities in terms of the products that can be obtained out of the biomass (such as petroleum-like fuels, hydrogen, fertilizer, and solid fuels). There are different technologies to obtain the desired products out of the biomass (such as biological, physical, and thermochemical conversions). Among the thermochemical technologies, pyrolysis and gasification have the advantages of being faster, cleaner and produce more valuable fuels than the other technologies. However, gasification and pyrolysis technologies are expensive and very sensitive to the process conditions.

To overcome the difficulties, research has focused on studying ways to enhance the efficiency of such systems by producing more valuable fuel and reduce operating cost. One of the most attractive solutions is co-pyrolysis and co-gasification, where different biomasses are mixed to have a combined effect that speeds up the reactions, increase the energy conversion, and reduce wear.

This thesis focuses on the study of co-pyrolysis and co-gasification of chicken manure and rice husk using two different approaches. The first approach is studying the co-pyrolysis and co-gasification kinetics between chicken manure and rice husk using Thermo Gravimetrical Techniques. A non-isothermal thermogravimetric analyzer, coupled with a differential thermal analyzer is used in this study. The second approach, based on a semiempirical model, was developed to predict the resulting gases of the process. This model is based on previous research and the kinetics of the thermochemical processes. Results show that adding rice husk can decrease the energy of activation in pyrolysis and gasification by up to 12%. For pyrolysis experiments, there was an increase in the degree of conversion up to 26% while for gasification the degree of conversion was increased up to 22%. The semi-empirical model gives a reasonable estimation of the syngas yields and composition for the individual biomasses. This model also predicts an expected reduction in the heating value of 12%.

TABLE OF CONTENTS

LIST OF FIGURES

LIST OF TABLES

LIST OF NOMENCLATURE

A	=	Frequency factor (min^{-1})
E_a	=	Energy of Activation (kJ/mol)
f_{bm1}	=	Biomass' mixing ratio
$k(T)$	=	Arrhenius Constant
n	=	Order of reaction
m_f	=	mass of fuel
m_{cf}	=	mass of carbon in the fuel
m_{of}	=	mass of oxygen in the fuel
m_{hf}	=	mass of hydrogen in fuel
m_{cch}	=	mass of carbon in the char
m_{och}	=	mass of oxygen in the char
m_{hch}	=	mass of hydrogen in the char
m_{ctar}	=	mass of carbon in the tar
m_{otar}	=	mass of carbon in the tar
m_{htar}	=	mass of hydrogen in the tar
R	=	Gas constant (8.314 J $mol^{-1}K^{-1}$)
T	=	Temperature (°C)
t	=	time (s)

w	=	Instantaneous mass (kg)
w_f	=	Final mass (kg)
w_o	=	Initial dry mass (kg)

Symbols

α	=	Extent of reaction
α_{bm1}	=	Degradation of chicken manure
α_{bm2}	=	Degradation of rice husk
α_{cal}	=	Degradation of the biomass mixtures
β	=	Heating rate (°C/min)

Abbreviations

AAEMS	=	Alkali and Alkaline earth metals
DTA	=	Differential Thermal Analysis
DTG	=	Differential Themo gravimetrical curve
ER	=	Equivalency ratio
LHV	=	Lower Heating Value
TG	=	Thermogravimetric curve
TGA	=	Thermo gravimetrical Analysis

1. Introduction

Energy is one of the main assets in today's economy. Energy consumption it is one of the factors that affects the wealth and economic growth of a country. Current electricity generation in the United States in 2020 is mainly based on fossil fuels with approximately of 61% of the share, with 19% of the share representing nuclear power [1]. However, due to the fluctuating cost of oil and natural gas (along with agreements to reduce carbon dioxide emissions) drive plans in the United States to increase the demand for renewable energy. Consequently, interest in alternative and renewable energy sources has been heightened. In 2020, electricity generation was 19% from renewable sources and it is expected to take 36% of the share by 2050 [1]. Biomass is one of the alternatives to meet the increasing energy demand that is increasingly being considered because it is abundant, carbon-neutral and clean. Biomass is defined as every organic source that can potentially be converted to energy [2]. Biomass can be classified into first, second, and third - generation biomass.

First-generation biomass includes starches and carbohydrates (e.g., corn or sugar cane). Generating fuels with this type of biomass requires growing plants that can be used as food. In addition, first generation biomass offers small benefit from the greenhouse standpoint because significant amount of energy is required to grow, collect and process the biomass [3].

Second generation biomass includes agricultural or animal waste - making it the most attractive biomass source because converting this kind of biomass into more useful products also reduces the greenhouse gases caused by the feedstock. Gerber estimated that the feedstock sector caused 14.5% of all human-caused greenhouse gasses emissions [4]. Third generation biomass typically refers to algae that can be transformed into bio-oils [5]. Algae has the advantage of rapid

growth, and also algae grows in not cultivable land and wastewater. Thus, algae do not compete for food production.

Biomass can be converted into bioproducts in three ways: physical, biological, and thermochemical conversion [6].

- In physical conversion, mechanical forces are applied to change the size and shape of the fuel. Typical configurations are pellets, chips, and powders. This conversion is typical to prepare the solid fuel for a further thermochemical or biological conversion.
- Biological conversion is based on the degradation of biomass using biological agents that decompose the waste and release energy. Abundant research can be found regarding processes such as anaerobic digestion or hydrolytic fermentation [6-9]. Biological conversion is a relatively inexpensive solution. However, biological conversion has high residence times, low conversion, and the conversion is very sensitive to the operating conditions. Also, the biosolids need proper disposal or those biosolids can cause health problems.
- Thermochemical conversion uses heat to promote chemical reactions that degrade the biomass. Recently, researchers' interest in thermochemical conversion has increased due to lower residence times, higher quality fuels, and higher conversions. Compared to the biological process, these thermochemical processes are an attractive solution to meet the increasing demand for renewable fuels. Literature has focused on five main technologies: torrefaction, pyrolysis, gasification, hydrothermal liquefaction, and combustion. The differences between these technologies are essentially the temperature, pressure, and residence time [6].

1.1 Studied feedstocks in the state of Wisconsin

Chicken's consumption in the United States has drastically increased over the past years. According to the National Chicken Council, the consumption of chicken per capita was estimated at 93.5 Lb per year [10]. The population in the state of Wisconsin is 5.8 Million. Using this statistic, the average estimated consumption of chicken in the state of Wisconsin is 542 M Lb of chicken per year. Considering that the average weight of a chicken is 3.5 lb, the state of Wisconsin likely consumes approximately 155 Million chickens per year. Each chicken releases roughly 2.5 lb of manure throughout their growth period. Thus, the amount of chicken consumed annually by the state of Wisconsin produces approximately 388 M lb (176 million kg) of manure per year. The heat value of chicken manure is approximately 14 MJ/kg, leading to an energy equivalent to that of 401,556 barrels of oil.

When chicken manure is stored away from farms (as it often is), harmful bacteria grows unchecked in a dangerous manner. Thus, storing chicken manure is not a feasible solution due to the health problems that bacterial growth may cause. In order to avoid this complication, chicken manure should be converted into energy as soon as possible.

An alternative biomass to chicken manure is rice husk. Annually, the United States produces approximately 5.6 million metric tons of rice [11]. Rice production's major by-product is rice husk. Rice husk is a protective layer in the rice that protects the grain during the growing season. Each kg of white rice leaves about 0.28 kg of rice husk. The consumption of rice per person in the united states is approximately 26 lb (12 kg) per year [11]. As such, the state of wisconsin produces approximately 19.5 million kg of rice husk annually. Rice husk has a heating value of 16 MJ/kg, resulting in approximately 50,949 barrels of oil equivalent energy.

2. Literature review

2.1 Introduction

Historically, direct combustion of biomass has been the most widely used method to extract energy from biomass. Direct combustion is an attractive solution due to the abundancy of biomass, flexibility, high efficiency, and availability when-needed [12]. However, only a few types of biomass can be used as fuel. Combustion of biomass can cause technical problems such as corrosion, secondary waste, and necessary treatment of the exhaust gases. Also, the low energy value of the biomass requires large volumes of fuel. Co-combustion of biomass with other fuels (such as coal), waste (such as plastics), or agricultural waste has been largely investigated [12-14].

The process of gasification to produce fuels has been used for approximately 200 years. The primary purpose of early gasification was to produce gas from coal and coke for lighting and heating purposes [15]. Then, when the internal combustion engine was invented, power cycles became more popular and the production of electricity brought an increase in the use of petroleum as fuel. With these advances, gas lines that were used for lighting were replaced by electrical ones. Consequently, the gasification process was no longer used. However, during the world wars, especially World war II, gasifiers were extensively used for vehicles due to difficulties regarding access to petroleum and coal [16].

After the war ended, the interest in biomass decreased because petroleum-based fuels had greater advantages than those of the gasification process: energy value was higher, maintenance easier, and there were better flow characteristics. These advantages made gasification undesirable. However, after the 1973 embargo caused petroleum prices to skyrocket, gasification gained interest to fill part of the energy gap. In the last 30 years, the increase and volatility in gas and

petroleum prices has increased the interest in gasification. Sasol Synfuels develop two remarkable gasifiers named “Sasol II” and “Sasol III” that produce syngas (CH_4, H_2, CO) since the mid-80s. [17]. Currently, research aims to improve the gasification process.

Pyrolysis can be traced back to ancient Egypt, when wood was pyrolyzed to produce tars for boats [18]. Pyrolysis studies were initiated in the 19^{th} century in France. Initially, studies reported the effect of different reaction conditions in the yield of solid, liquids, and gases [16]. Pyrolysis was used to produce charcoal with a heating value similar to coal [19]. However, after other fuels took more relevance and carbon extraction became cheaper, pyrolysis had little progress until the 1960s. During that era, kinetics was the main focus. Friedman developed a model based on the Arrhenius equation to describe the kinetics [20]. Roberts [21] studied the kinetics of wood, comparing laboratory-scale experiments with larger-scale experiments, and concluding that pyrolysis follows different routes depending on external factors, resulting in a significant variation of the pre-exponential factor.

After the 1980s, research aimed to optimize the yields of gas and biosolids, and also focused on the improvement of pyrolysis reactors [19]. Several researchers have aimed to improve thermochemical processes by using certain chemicals as catalyzers- such as alkali and alkaline earth metals (AAEMS), zeolite and acids. AAEMS were shown to improve the biochar yields for pyrolysis, while for torrefaction AAEMS increased the energy density, heating value, grindability and degradation properties. For gasification, Ong et al. proved that AAEMS produce an increase in the hydrogen content [6].

2.2 Biomass composition

The principal constituent of biomass is Carbon C, comprising from 30-60% of the dry matter content. Typically Hydrogen and Oxygen comprise between 1-45% and nitrogen concentrations are relatively low [22-25].

Biomass' C, H, O, N is assembled in three major components - cellulose, hemicellulose, and lignin. However, the proportions of these components vary based on the type of feedstock. Greenhalf [26] showed that biomass with higher lignin content degraded in a wider temperature range and produce higher energy value bio-oils.

Cellulose is a polysaccharide based on linear chains of glucose units. It is an important structural unit for plants and organic matter. Cellulose is approximately 40-60%wt of the total biomass component [25]. The chemical formula of cellulose is $(C_6H_{10}O_5)_n$, where n is the degree of polymerization. The degree of polymerization indicates how many units of glucose are bonded. Mettler [27] studied the effect of the degree of polymerization in the pyrolysis, concluding that the degree of polymerization has little impact over the product composition. However, higher degrees of polymerization lead to higher yields of products. Cellulose can be crystalline or amorphous; crystalline cellulose has better thermal stability and it degrades at higher temperatures compared with amorphous cellulose.

Hemicellulose is a heteropolymer that consists of glucose and several sugars produced during photosynthesis (such as xylose and arabinose). The composition and degree of polymerization of hemicellulose vary significantly depending on the feedstock. Hemicellulose is composed of shorter molecules than cellulose [28]. Hemicellulose presents an amorphous and branched structure [29]. Depending on the feedstock, hemicellulose can cover from 15-30% wt.

Lignin is a natural polymer made from phenol (aromatic matrix) units with strong intramolecular bonding. Lignin is an essential structural material in the support tissues of vascular plants and some algae. The thermal degradation of lignin covers a wide range of temperatures because there are different ways that the phenol can bond internally, such as ether linkage (that can cleave at low temperatures) or carbon-carbon bonds (which are more stable and break at higher temperatures). Lignin can reach from 10-25% of the total dry biomass [15,27].

Biomass also contains small amounts of inorganic materials (such as calcium, silica, phosphorous or metallic materials). The ashes reveal the composition of inorganic materials. Calcium Oxide (CaO) is the main component in wood biomass' ash [30]. SiO_2 is the major component in agricultural biomass [31]. This inorganic material can enhance the degradation of biomass when the inorganic material acts as catalyzers.

2.3 Pyrolysis of biomass

Pyrolysis is a series of thermally driven reactions that decompose the organic material. Degradation of biomass can be divided in three main steps: drying, primary pyrolysis, and secondary pyrolysis. Each process degrades a different component. Thus, the yield is different for each step. Figure 1, shows a schematic for the degradation of biomass. Moisture varies between 5-20% for agricultural and animal waste [32]. The remaining water is bonded to the biomass and this water is extracted during the pyrolytic evaporation process.

Primary pyrolysis happens at temperatures from 250°C to 600°C. This stage breaks down the bonded water, hemicellulose, cellulose, and lignin in the biomass, releasing some pyrolytic gases and condensable liquids. The remaining solid mass is known as biochar. The main pyrolysis mechanism is thermal cracking, when the long chains of cellulose, hemicellulose, and lignin break down into smaller hydrocarbons, hydrogen, and carbon.

The residual biochar is a component high in carbon that is not ideal to use as a fuel due to the incompatibility with biofuels from transportation, handling, and ashes. Nonetheless, biochar can be used in agriculture as soil amendment, carbon sequestration and activated carbon [33].

The liquid product that results from pyrolysis is known as bio-oil; the bio oil can be brownish-yellow to dark brown. Tar is mainly composed of aromatic alkenes and phenols. Bio-oils are the most preferred output from pyrolysis because bio-oils are easy to transport and can be compatible with the biofuels used in the transportation sector [33].

Several factors affect the yield of products. According to the operating conditions, pyrolysis can be classified as slow pyrolysis, fast pyrolysis, or flash pyrolysis.

- Slow pyrolysis uses long residence times (5- 30 min) and low heating rate(<10°C/s). This slow process ensures that the pyrolysis reactions are completed, increasing the yield of biogas [34].
- Fast pyrolysis uses faster heating rates (<100°C/s) and residence times from 0.5 to 2 seconds. This method maximizes the yield of bio-oils. One disadvantage of this method is the necessity of small particle size to ensure temperature uniformity.
- Flash pyrolysis uses very short residence times (<0.5 seconds) and higher heating rates (>500°C/s). This process is aimed towards the production of mainly liquid bio-products [35].

The decomposition of hemicellulose, cellulose and lignin in woody biomass has been studied using the differential scanning calorimeter (DSC) by Yang [36]. Results show that at temperatures below 400°C, the pyrolysis of cellulose is highly endothermic. However, for hemicellulose and lignin, the dominant reactions are exothermic. At higher temperatures, the

opposite behavior was observed. Cellulose pyrolysis becomes exothermic and lignin and hemicellulose become endothermic. Cho [37] studied the kinetics and heats of reaction for pyrolysis of solid cellulose, finding that the reactions that form char, carbon dioxide, and water are exothermic.

2.4 Gasification

The gasification process targets maximizing the conversion of solid feedstock to obtain gases such as H_2, CH_4,CO, C_2H_X, and C_3H_x. The main difference between pyrolysis and gasification is that in gasification the feedstock comes in contact with a gasifying agent (such as air) at high temperatures (800-1400°C)[16], while in pyrolysis the atmosphere is inert.

In contrast to combustion, gasification uses controlled amounts of oxygen added into the gasifying agent. This agent will promote reactions that partially oxidize and reduce the biomass, yielding syngas and leaving ashes as a solid by-product of the process.

Among the gasifying agents, CO_2, H_2O, O_2 and air are widely studied. Air gasification has the advantage of being cheap and easy to implement. The steam gasification of biomass is abundantly studied, resulting in proof that steam gasification yields syngas with a high energy value [38]. However, steam gasification is expensive and harder to control. Pala [39] developed a model to study the yields of hydrogen. In this study the temperature increase decreases the yields of methane and carbon dioxide through the reverse methanation and the Boudard reaction respectively. Chaudhari studied the steam gasification of biomass to produce syngas. Results show that the combination of the lowest steam flow rate, lower temperature and lower residence time gave ratios H_2/CO ideal for Fisher-Tropsch synthesis. While higher energy valuable fuel can be obtained with higher temperatures and higher heating rates [40].

In air gasification, to ensure partial oxidation of the biomass, the equivalence ratio (ER) is kept within a range from 0.2 to 0.4 [41]. Cheng et al. [42] concluded that mixing 60% CO_2 (mass percentage) with air gasification lead to maximum CO and CH_4 yields. Oxygen gasification is used to solve the inconvenience of syngas dilution caused by nitrogen in air. Zhou [43] found that the optimal oxygen to biomass ratio is 0.4 and adding more oxygen would decrease the heating value of the syngas.

Some studies focused on mixing gases to reduce the cost of operation, increase the yield, and open opportunities for heat recoveries. Hussein [44] showed an improvement of carbon conversion when oxygen is added to the steam gasification of chicken manure.

Every gasification process follows four steps: drying, pyrolysis, oxidation, and reduction. The main reactions for gasification can be found in Table 1 [41]. Gasification has the advantage of providing syngas free of contaminants without any additional treatment.

Oxidation is a highly exothermic reaction that is essential to decrease the amount of tar generated. Different models have attempted to approach the kinetics of the oxidation. In the reduction part, gasification takes place in several reactions (such as a water-gas reaction or Boudouard reaction) that yield hydrogen, carbon monoxide and methane as described in Equations 2,3, and 5. These reactions occur at high temperatures (700 K) and are highly endothermic, limiting the temperature control in the reaction. Note that some reactions (water shift reaction and methanation) use water vapor to obtain more desirable gases on the syngas (methane and hydrogen).

Table 1 Gasification Reactions

Reaction	Formula	H @ 298 K (kJ/mol)	Eq.
Thermal Craking	$C_nHm=C+H_2+C_xH_y$	-varies	(1)
Boudouard reaction	$C+CO_2=2CO$	172	(2)
Water- gas reaction	$C+H_2O=CO+H_2$	131.4	(3)
Methanation reaction	$C+2H_2=CH_4$	-75	(4)
Water-gas shift reaction	$CO+H_2O=CO_2+H_2$	-41	(5)
Carbon dioxide dissociation	$2CO_2=2CO+O_2$	532	(6)
Oxidation of carbon	$C+O_2=CO_2$	-393.8	(7)
Oxydation of Hydrogen	$H_2+1/2O_2=H_2O$	-242	(8)
Oxidation of carbon monoxide	$CO+O_2=CO_2$	-283	(9)

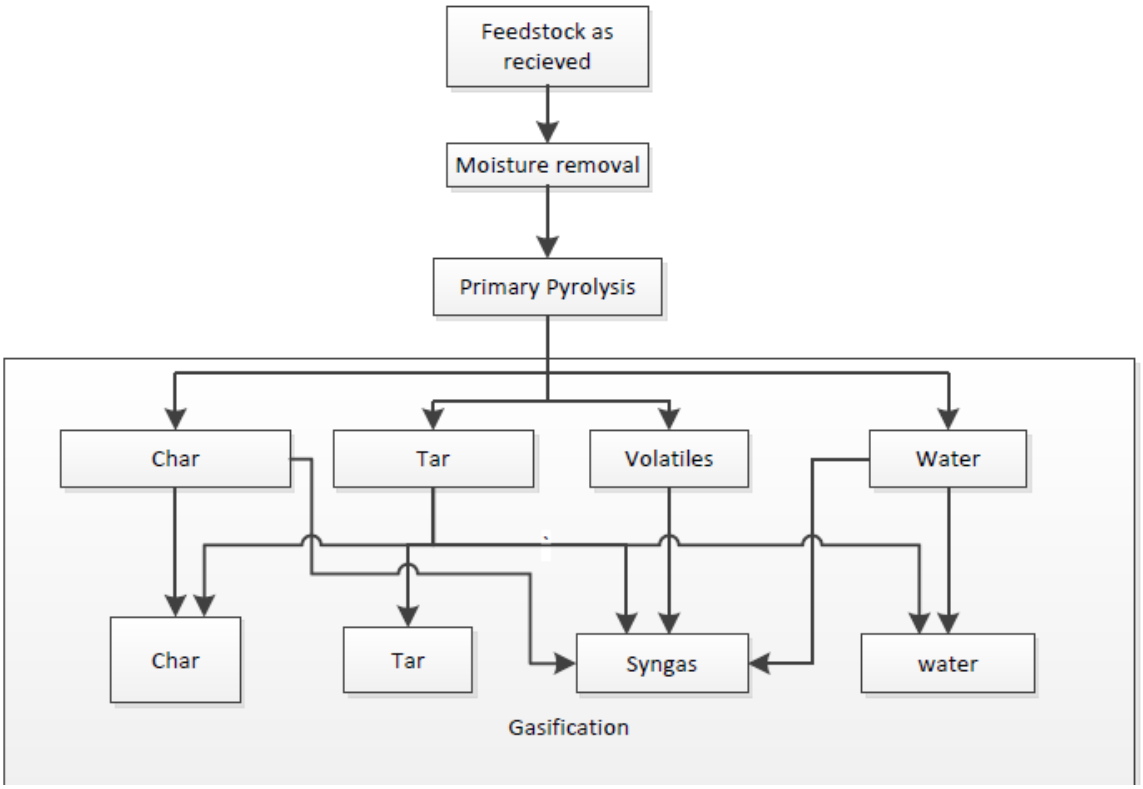

Figure 1 Pyrolysis-gasification process

2.5 Co-pyrolysis and Co-gasification

Co-pyrolysis and Co-gasification are viable options to apply thermochemical conversion technologies for biomasses that, on their own, have poor performance when decomposed individually but perform better when mixed with another fuel.

Research has focused on mixing lignocellulosic biomass with solid fuels such as coal [45,46]. Results show that some biomasses can produce positive synergetic effects, increasing the yield of volatiles without affecting the process. He [47] mixed cotton and coal. Results showed that the rate of decomposition was increased for the co-pyrolysis blends. Also, mixing biomass can yield to higher production of AAEMS and a lower energy of activation was reported as a result.

Researchers further studied mixing biomass with plastics [48]. Results show that the co-pyrolyzed waste samples give better quality and higher quantity syngas when compared to the standalone biomass pyrolysis [49,50]. Polymers have high hydrogen contents and, consequently, provide hydrogen during the co-pyrolysis process. A significant interaction between the two feedstocks causing mass reduction, volatile generation, and overall energy usage reduction (depending upon the ratio of plastics in the mixed blends) [51].

In addition, researchers are endeavoring to convert rice husk into higher-value efforts [52,53]. Hossain et al. [54] studied the co-pyrolysis of a solid tire with rice husk to show the possibility of obtaining liquid products that are comparable with petroleum fuels. However, these liquid products are only produced if the pyrolysis conditions are correctly selected. Costa et al. [55] investigated mixing the rice husk with plastic waste using different pressures and residence time. Results show an enhancement in the biomass conversion. Also, the best performance was obtained with lower pressure and higher temperatures and shorter residence times, or lower pressure, lower temperature, and higher residence time.

Guo et al.[56] demonstrated that extractives in singular biomasses could improve the thermal degradation of hemicellulose and cellulose when combined with other biomasses' extractives. Mallick et al.[57] showed that the binary conversion of the biomass, depending on the blend ratio (without considering any synergetic effects), can be estimated as:

$$\alpha_{cal} = (1 - f_{bm1})\alpha_{bm2} + f_{bm1}\alpha_{bm1} \qquad (10)$$

Where f_{bm1} is the mass ratio, and α_{bm1}, α_{bm2} are the conversions for the primary and secondary biomasses.

Dayananda et al. [58] studied Co-gasification of chicken litter with rice husk experimentally. Results show a negative correlation between the equivalence ratio and the heating value, meaning that higher equivalence ratio yields lower quality syngas. Also, the mixture with 30% rice husk was reported to yield the best quality producer gas.

2.6 Pyrolysis and gasification reactors

The thermochemical processes occur inside a reactor. There are several types of reactors. The most common types of reactors are: (1) batch reactors - where the raw fuel is decomposed in batches;(2) moving bed reactors - where biomass is decomposed constantly ;(3) reactors with movement caused by mechanical forces and, (4) reactors where the movement is caused by fluid flow (fluidized bed) [33]. Moving bed and fluidized bed reactors are largely investigated and documented [59] because such reactors offer more flexibility for the fuel type, allowing the gasification of various biomasses without many changes [60]. However, rotary reactors (group (3)) are currently gaining popularity because the rotating action ensures rapid heat transfer. For instance, Wagennar et al. [61] experimentally showed that the rotating cone reactor is capable of fully pyrolyzing the biomass without using carrier gas.

2.7 Thermal Gravimetrical Analysis (TGA)

The thermal analysis started in 1887, when Le Chatelier published a paper associating chemical reactions of clay with temperature [62]. Thermal analysis has three main branches: Cooling Curve Methods, Thermogravimetric Analysis, and Differential Thermal Analysis.

Thermogravimetric analysis measures the mass changes caused by the cooling or heating of the substance under certain atmosphere at a specific heating rate. The typical thermal decomposition of biomass involves different simultaneous reactions of organic materials.

Nonetheless, overall kinetic reaction parameters can be obtained through Thermal Gravimetrical Analysis (TGA) [63]. Every model studying the kinetics is based on the Arrhenius equation.

$$k(T) = Ae^{-\frac{E_a}{RT}} \qquad (11)$$

Where A is the pre-exponential or frequency factor that is considered constant, E_a, is the energy of activation, R is the gas constant, and T is the absolute temperature. $k(T)$ is the temperature-dependent reaction rate constant (or Arrhenius constant).

The energy of activation can be understood as the energy needed for the molecules to start a reaction. The preexponential factor measures the frequency at which the molecular collisions occur. Therefore, $k(T)$ gives the frequency (rate) of successful molecular collisions [63].

The kinetics of biomass is usually expressed as a single reaction, under isothermal conditions the decomposition rate of biomass can be obtained by multiplying the rate of reaction $k(T)$, by the mass conversion $f(\alpha)$

$$\frac{d\alpha}{\mathrm{d}t} = k(T)f(\alpha) \qquad (12)$$

Combining Eq. (11) and Eq. (12), the following expression is obtained:

$$\frac{d\alpha}{\mathrm{d}t} = -A\mathrm{e}^{-\frac{E_a}{RT}} f(\alpha) \qquad (13)$$

where, α is the degree of conversion or extent of reaction, which can be expressed in terms of the initial dry mass, the final mass, and the instantaneous mass, as shown below:

$$\alpha = \frac{w_0 - w}{w_0 - w_f} \qquad (14)$$

$\frac{d\alpha}{dt}$ represents the rate of change of mass, and $f(\alpha)$, where $f(\alpha)$ is a conversion function that describes how the biomass is decomposed, $f(\alpha)$ changes depending on the kinetic model used. For biomass, an n-th function order is commonly used [63]. Thus,

$$f(\alpha) = (1-\alpha)^n \qquad (15)$$

Where, n is the order of the reaction. The devolatilization of biomass is often expressed as a first-order reaction. Thermogravimetric analysis experimentally can be conduct in two different techniques, isothermal-techniques, and non-isothermal techniques.

Isothermal techniques evaluate the mass change of the solid with time under a constant temperature; non-isothermal experiments change the temperature at a constant rate known as heating rate. Non-isothermal techniques are easier to carry out because the sample does not do a sudden temperature jump [64].

For non-isothermal methods, the rate of change of conversion can be expressed as a function of temperature as shown:

$$\frac{d\alpha}{\mathrm{d}t} = \frac{d\alpha}{dT}\frac{dT}{dt} \qquad (16)$$

where $\frac{dT}{dt}$ is the heat rate, which is commonly expressed as β.

Isoconversional methods (also called model-free methods) assume that conversion and/or temperature remains constant. Isoconversional models do not require previous knowledge of the reaction mechanism in the thermal degradation. Isoconversional models can follow differential or integral approaches. Differential approaches (such as Friednman model[20]) directly use the Arrhenius equation. Integral approaches - such as Kissinger-Akahira-Sunose (KAS) or Flynn Wall-Osawa (FWO) [65] - require numerical integration of the function $f(\alpha)$ (see Eq. 17) leading

to truncation errors. On the other hand, differential methods are very sensitive to noise, giving inconsistent results. However, the noise inconvenience can be resolved by using smoothing data techniques [66]. Wang [67] showed that differential isoconversional methods are more accurate than integral methods, but more than one test must be run to ensure accuracy.

$$g(\alpha) = \int_0^{Ta} \frac{d\alpha}{f(\alpha)} = \frac{A}{\beta} \int_0^{Ta} \exp\left(-\frac{E_a}{RT}\right) dT \quad (17)$$

The Friedman method directly uses Eq. (13). Taking logarithm and rearranging as follows [20]:

$$ln\left(\frac{\frac{d\alpha}{dt}}{(1-\alpha)^n}\right) = ln\left(-\frac{A}{\beta}\right) - \frac{E_a}{RT} \quad (18)$$

Thus, by plotting the left-hand side of Eq. (7) and 1/T, it results in a straight line with a slope of $(-\frac{Ea}{R})$, and an intercept with the y-axis of $\ln\left(-\frac{\mathrm{A}}{\beta}\right)$. This method is more reliable when the biomass is tested under several heat rates, and the kinetic parameters are averaged.

Gaur et al. [68], compiled the thermogravimetric data for multiple biomasses in an atlas for different fuels. Kim et al. [69] studied the pyrolysis characteristics of chicken litter (woodchips, broiler, and flock manure) using thermogravimetric analysis and the Friedman model with a first reaction order. Lim et al. [70] described the kinetics of rice husk using thermogravimetric analysis at four different heat rates. The kinetic parameters were described using the KAS method and the results of this method showed an increase in the degradation with the heating rate. Sobek [71] described pyrolysis' kinetics of waste wood in a solar reactor using typical heating rates reported for these types of reactors. Results show that the major mass loss and condensable release occurs at temperatures between 250 and 440°C. The major release of H_2 occurs at a temperature of approximately 709°C.

Hussein [17] and Selim et al. [72] studied the kinetics of pyrolysis and gasification of chicken manure using nitrogen, air, steam and carbon dioxide. Different orders of reaction were found for each reaction.

2.8 Pyrolysis and gasification products

As previously explained, pyrolysis and gasification yield char, syngas tar, and ashes. As such, the overall mass balance for the process can be defined as below:

$$m_{biomass} = m_{char} + m_{gas} + m_{tar} + m_{ash} + m_{moisture} \quad (19)$$

Where,

$$m_{gas} = m_{H_2} + m_{CH_4} + m_{CO} + m_{CO_2} + m_{C_xH_m} + m_{H_2O} \quad (20)$$

Researchers have focused on describing the yields of each component for different kinds of biomass [17,26,46,73]. Literature shows that peak temperature is one of the main factors affecting the yields of syngas and tar. Generally, the increase in temperature increases the yield of syngas, and decreases the yield of char and tar.

The yields of syngas are frequently expressed on a dry fuel basis. Some researchers [21,74] developed relationships between the yields of CH4 and CO, the yields of H2 and CO, and hydrogen yields depending of the temperature. Results indicate that H_2 and CO are related by a power function dependent of the temperature; CH_4 and CO linearly correlate, and H_2 follows a power function depending on the temperature. Normally the yields of heavier hydrocarbons (such as C2H6, C2H4, C3H8) are combined into a single group due to low concentrations of the syngas. CO_2 is one of the main components in the syngas. CO_2 is formed at all stages of pyrolysis.

However, higher CO_2 concentrations can be found at early stages of pyrolysis and its higher abundance for hemicellulose and lignin [36].

The maximum yield of tar is obtained at medium temperatures. Literature shows that increasing the temperature more than 500°C can decrease the formation of tar due to the start of secondary pyrolysis [73]. Tar yields are often collected for fast pyrolysis processes. However, for slow pyrolysis the tar yield usually is not reported.

The energy balance for the process uses the pyrolysis system as the volume control. The inlets of the system are the biomass and heat (electricity). The outputs are syngas, char and bio-oil.

$$E_{fuel} + E_{heat} = E_{syngas} + E_{biochar} + E_{biooil} \qquad (21)$$

Where the energies on the syngas or bio-oil can be calculated as

$$LHV_t \times m_t = \sum LHV_i \times m_i \qquad (22)$$

Where m_t is the mass of gas or tar, i represents each component. LHV represents the lower heating value of each component. The upper side term in equation 21 can be seen as the total energy extracted. The energy on the fuel can be estimated as the mass of fuel times the lower energy value.

2.9 Differential Thermal Analysis (DTA)

Differential thermal analysis is a thermal analysis technique that uses a reference to measure temperature differences. The sample and the reference are heated inside a furnace. The difference in temperature between the reference and the sample is recorded with time. The difference in temperature indicates if the reactions are endothermic (negative temperature

difference) or exothermic (positive temperature difference). After each reaction is complete, the temperature difference decreases – leaving a peak – and each peak represents a characteristic of the reaction.

DTA is widely used in material science to determine characteristic temperatures in phase diagrams. Rieger [75] used DTA to determine and compare the glass transition temperature in different polymers. DTA has also been used for fuel characterization. Glass [76] characterized different coals depending on the magnitude of the endothermic peaks. Results concluded that the higher endothermic peaks were considered lower grade of the coal (meaning that more energy must be provided to covert such coals). The coals were classified as meta-anthracite, anthracite, low volatile, high volatile and bituminous.

3. Experimental set up and procedure

3.1 Shimadzu DTG 60H

To run experiments the Shimadzu DTG 60 H is used (see Figure 2). This device can measure the changes in mass (TG) and temperature difference (DTA) simultaneously. The main components of the DTG are: (1) the furnace, where the samples are loaded; (2) the thermal analysis workstation TA-60 WS; and (3) the atmosphere gas controller FC 60-A.

1. The furnace consists of an electrical heater that provides heat to the chamber. The furnace can operate to a temperature up to 1500℃. Inside the furnace two rods (fitted with thermocouples pt10%Pt/Rh) rest on a sensitive balance mechanism (Roberval mechanism) where the mass of the sample is compared with a reference. Using this balancing mechanism ensures that the position of the mass does not affect the measures, also the baseline drifts caused by buoyancy or convection are minimized [77].The measurable mass range is ± 500 mg with readability of 0.1 μg. The DTG can measure a mass up to 1 g in gross weight (including tare weight). The thermocouples measure the temperature in the reference and the sample, the temperature difference is expressed as a voltage difference in μV ensuring a precise reading. The measurable voltage range for the DTA is $\pm 1000 \mu V$

The furnace has an auto-sampler which is a robotic arm that automatically loads-unloads the samples and runs the experiments according to the program. The autosampler has a capacity of 24 samples.

The furnace is also equipped with a cooling fan that provides short and efficient cooling times. For safety reasons the furnace does not open at temperatures higher than 150°C.

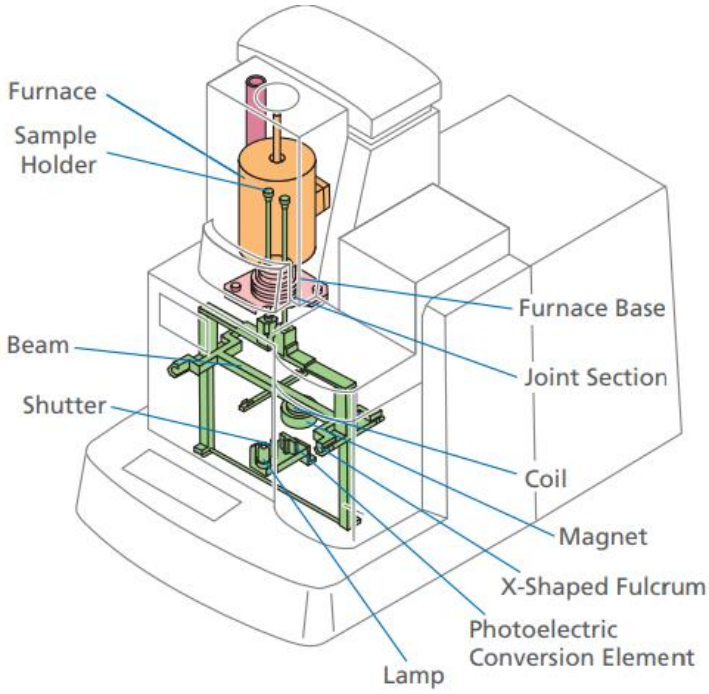

Figure 2 DTG experimental set up

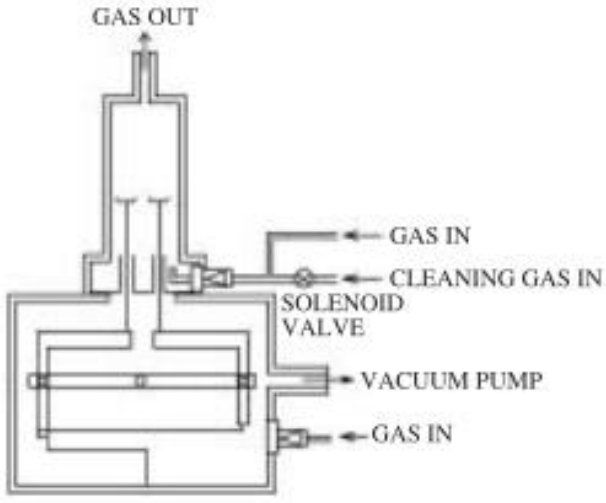

Figure 3 Side view of the DTG

Figure 4 DTG 60-H detectors

2. The thermal analysis workstation TA 60WS serves as an interface between the DTG and the PC. This device can be understood as the brain of the DTG. The TA-60WS can control the temperature programs, gas flow rates, atmosphere control and displays the data.

3. The atmosphere gas controller, or the FC-60 A, is used to control the flow rate of the purge and reacting gas. The flow rates can be controlled manually or in the software. The purge gas (Nitrogen) must flow inside the furnace all the time to avoid reactions that can damage the balance of the mechanism. The FC-60 A allows the use of two gases including the purge gas. If more than two gases must be mixed, the gases should be mixed separately.

Figure 5 Flow controller

Procedure

The biomass was first ground manually. Scanning electron microscopy (SEM) model JSM-IT800 was used to measure the average dimensions of the samples, the dimensions are described in the next section. The procedure for DTG experiments is as follows:

1. Load an empty cell in the furnace. Check for any zero error and reset until zero mass and zero voltage are reached.
2. With an empty furnace, run nitrogen at 50°C for ten minutes to purge the furnace.
3. Put the sample of the biomass. The sample mass was set to be 20 mg. An error of 1% was considered acceptable (19.9 mg to 20.1 mg). Blended biomass in ratios from 0 to 50 % of mass-based rice husk. 10 mg of rice husk were tested independently because the density of rice husk is much smaller than the density of the other two livestock.
4. On the software set the following parameters:
    - Temperature range: 100℃ to 1000℃, with a 15-minute step at 100°C. The dry mass is measure at 104°C to estimate the humidity content.
    - Pan Material: Alumina

- Reacting atmosphere: Air or Nitrogen at a flow rate of 100 ml/min,
- Data acquisition is taken with a frequency of 1 Hz.
- Heating rate varies from 5 to 15 °C/min.

For Pyrolysis experiments, the flow rate is 100 ml min^{-1} of nitrogen. For gasification the flow rate of nitrogen is 100ml min^{-1} and 5ml min^{-1} of air.

4. DTA and TGA results

4.1 Pyrolysis of Chicken Manure

Chicken manure is a lignocellulosic biomass, with 24% Hemicellulose, 12% Cellulose, and 2% Lignin [78]. The proximate analysis and chemical analysis is shown in Table 2. Chicken manure was found to be approximately spherical with an average ratio of 380μm (see Figure 6).

Table 2 proximate analysis and ultimate analysis of chicken manure

Proximate analysis	(%wt/dry)
Moisture content	9.74
Ash Content	26.33
Volatile content	58.97
Fixed Carbon	10.8
HHV (MJ/kg)	14.29
Ultimate Analysis	
Composition	Standart (%wt/dry)
C	34.51
H	4.79
O	26.31
N	3.42
S	0.74

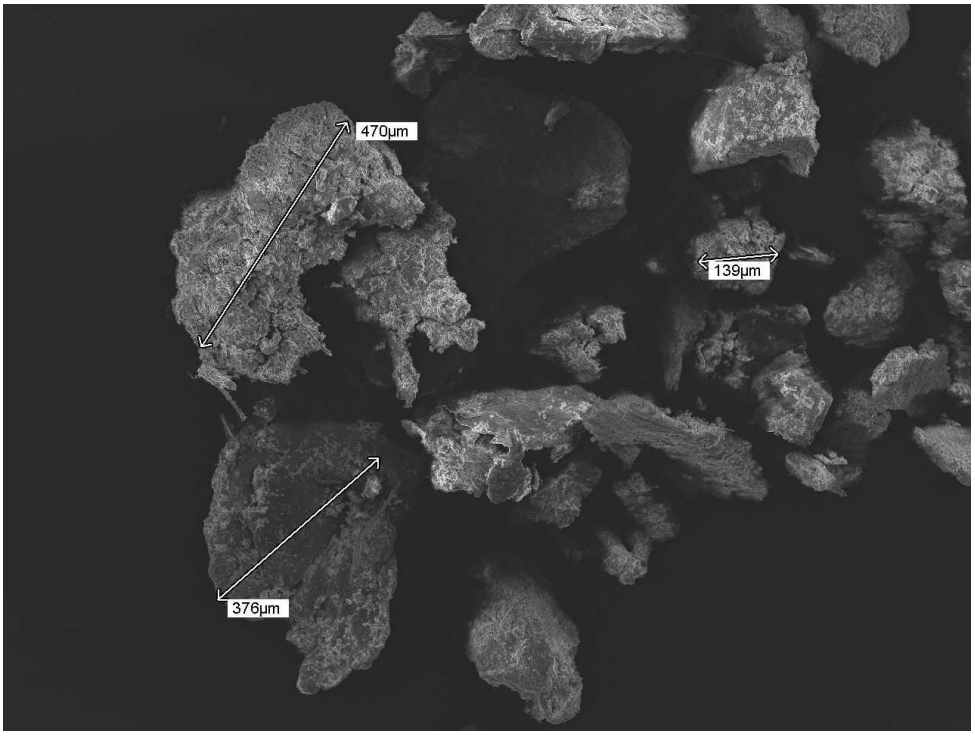

Figure 6 Chicken Manure SEM images (X50)

The Thermo Gravimetrical (TG) curves for chicken manure at different temperatures can be seen in Figure 7. The degradation of chicken manure can be divided into three stages. The first stage is from 100 ℃ to approximately 225 ℃. In this stage, evaporation takes place at temperatures up to 150℃. This stage represents a mass loss of approximately 10%.

Thermal cracking of biomass components occurs from 250-360℃. This is commonly known as the second stage of pyrolytic decomposition and corresponds to hemicellulose and cellulose degradation. This also corresponds to the lignin slowly beginning to decompose. Specific reactions cause the decomposition of these components. These reactions include: cracking the carbonyl and carboxyl groups (decarboxylation), cracking the methoxyl groups (methanation), and dehydration reactions. As such, high yields of CO_2, CH_4, CO, water vapor, and smaller yields of other organics (such as acids and aldehydes), are expected at this stage.

The Derivatives of the Thermogravimetric curves (DTG) are shown in Figure 8. As depicted, the trend is relatively stable, except at some peaks. The first peak occurs at temperatures from 257°C to 280°C, which corresponds to the peak thermal degradation of hemicellulose. The second peak appears at a temperature between 321°C and 340 °C, which typically corresponds to the degradation of cellulose [68]. The magnitude of the peaks increases when the heating rate increases; at the lowest heat rate, the peak of hemicellulose and cellulose are approximately 4.7×10^{-4} s^{-1} and 5.3×10^{-4} s^{-1}. With 15ºC/min, the magnitude of the first peak is approximately the same as the second (approximately 1.4×10^{-3} s^{-1}). When the heat rate is increased (5ºC/min), the magnitude of the second peak becomes more substantial than the first peak. The same behavior was observed by Hussein [17]. The pyrolysis of chicken manure occurs in several different reactions at a wide range of temperatures due to the lignin's slow decomposition and the complex nature of hemicellulose and cellulose.

The crystalline components of cellulose and lignin degrade during the 360-800℃ temperature range. This degradation occurs during the third stage of pyrolytic decomposition. In comparison to the prior two stages, the temperature range during the third stage is more vast and steadier, resulting in a slower rate of degradation. Before any remaining lignin and cellulose fully decompose, the stage reaches its peak of degradation at 730°C but no significant mass is lost after temperatures exceed 700°C. Similarly to the second stage, when the heating rate increases, the magnitude of the peak of the third stages' degradation rate increases. At lower heating rates the magnitude of this peak is irrelevant. At 15°C/min the decomposition rate is 1.8×10^{-4} s^{-1} (Figure 8).

The increase in the heat rate for all stages causes a delay in the mass degradation's progress to higher temperatures, and overall peaks in decomposition, because the reactions cannot be

completed before the temperature increases. As a consequence, the temperature needed for the biomass to decompose increases (as can be seen in Figure 7). Biochar remains after the process is completed. The biochar was found to vary between 34 and 40% wt, signifying that the total conversion for this biomass varied from 66% to 60% wt (Figure 7). The increased heating rate slightly shifted the curves to the right, thus decreasing the total conversion.

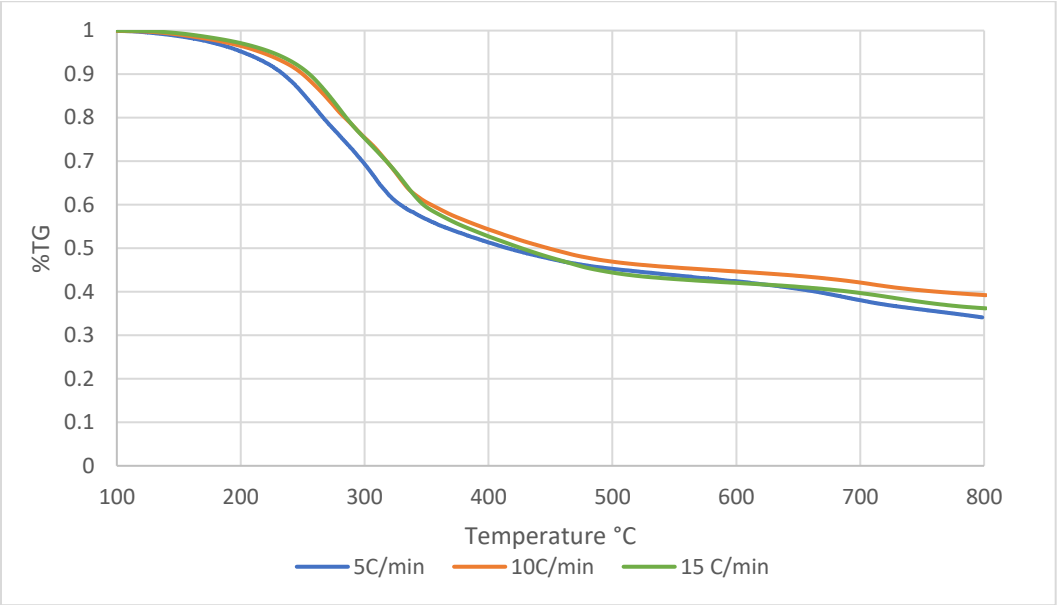

Figure 7 TG curves at different heat rates for chicken manure

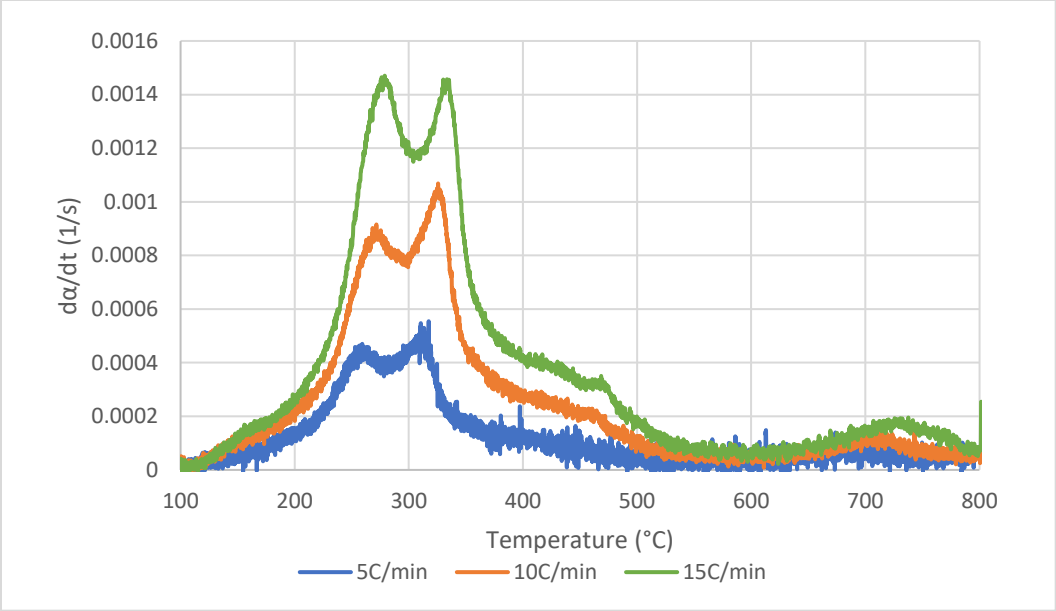

Figure 8 DTG curves at different heat rates for chicken manure

4.2 Pyrolysis of Rice Husk

Rice husk is a berlignoselulosa biomass with 50% of cellulose, 25-30% lignin, and 15-20% silica [79]. The chemical and proximate analysis can be found in [78]. Rice husk shape can be approximate to rectangles, where the length is almost twice the width, resulting in average dimensions of 727 µm × 363 µm.

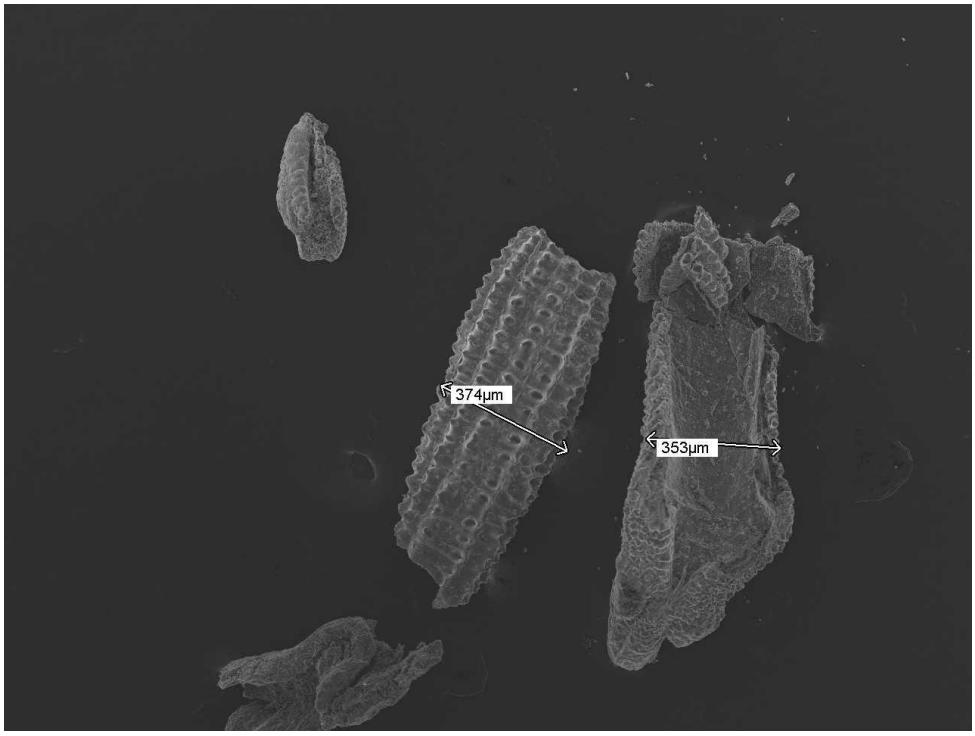

Figure 9 Rice husk SEM images (X75)

Table 3 Rice husk Properties

Proximate analysis	(%wt/dry)
Moisture content	11.2
Ash Content	18.29
Volatile content	48.31
Fixed Carbon	22.2
Ultimate Analysis	
Composition	Standart (%wt/dry)
C	27.92
H	4.23
O	37.86
N	0.49

No peak below 270 °C is expected because the degradation peak of hemicellulose is at temperatures between 240-270°C [68].

The mass degradation of rice husk can be divided into three stages. The first stage is the same as that for chicken manure - water is evaporated from 100°C to 225°C. Experiments showed a moisture removal of approximately 8%.

The second stage starts at approximately 250 °C and peaks at a temperature between 325°C and 350°C (depending on the heating rate). This peak corresponds to the degradation of the cellulose. In this temperature range, 50% of the biomass decomposes. At this temperature range a shoulder in the degradation curve is observed at 230°C. One reason for this result is the initial decomposition of cellulose and the initial stages for the degradation of lignin. These two early degradations are moved to higher temperatures when the heating rate is increased (explaining why, when the heating rate increases, the shoulder becomes less noticeable). The pyrolytic peak of rice husk is less distributed than the pyrolysis of chicken manure due to the absence of hemicellulose.

The third stage occurs within the 400°C to 650°C range. In this stage, the more stable components in the lignin decompose. The percentage of lignin in the studied rice husk decomposed entirely at this stage because there is no further peak degradation. Also, the lignin is more thermally stable than the cellulose, thus causing the slower degradation rates at this stage. The total conversion for this biomass is 60% wt, signifying that 40% of the biomass remained as biochar. (Figure 10).

When the heating rate is increased, the peak of the degradation rate and the temperature (at which the peak occurs) increases (Figure 11). At 5°C/min, the peak of rice husk decomposition is 9.9×10^{-4} s^{-1} while at 15°C/min the decomposition is 2.98×10^{-3} s^{-1}. The heating rate effect on rice husk's decomposition is the same as the effect obtained for the chicken manure case in Figure 8. It can also be observed that the DTG curve has only one dominant peak, which takes place at 325, 340, and 350°C, for the 5, 10, and 15°C/min heating rates, respectively. A plausible reason for that

result is that the rice husk has more cellulose content than hemicellulose and the lignin's slow decomposition rate.

When the heating rate was increased, the TG curves shifted slightly to the higher temperature side in the second stage but merged in the third stage - leading to almost identical conversions. This indicates that the third stage of decomposition is more thermally stable than some other stages.

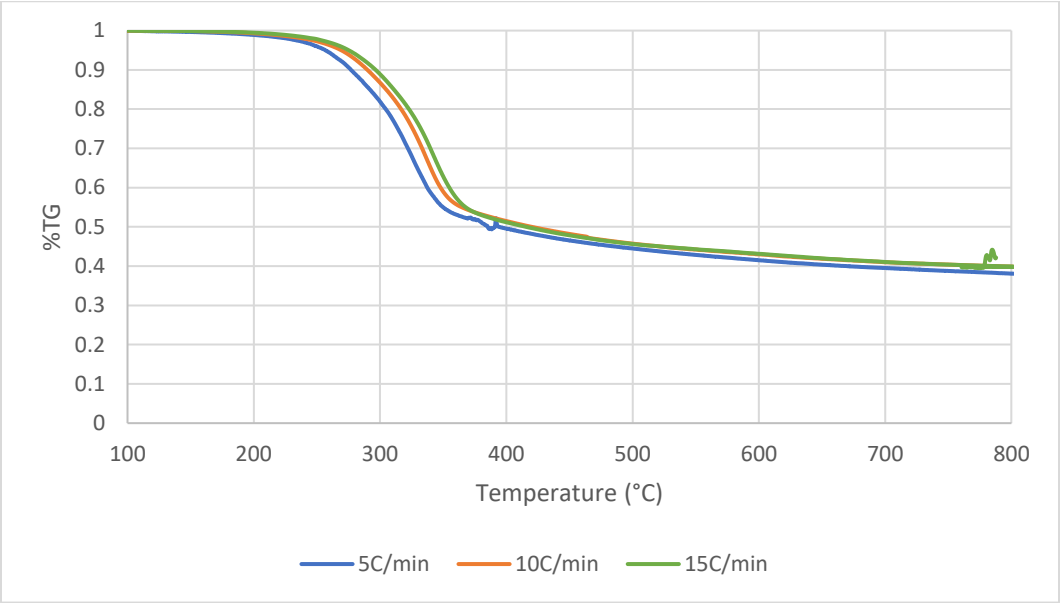

Figure 10 TG curves for rice husk at different heat rates

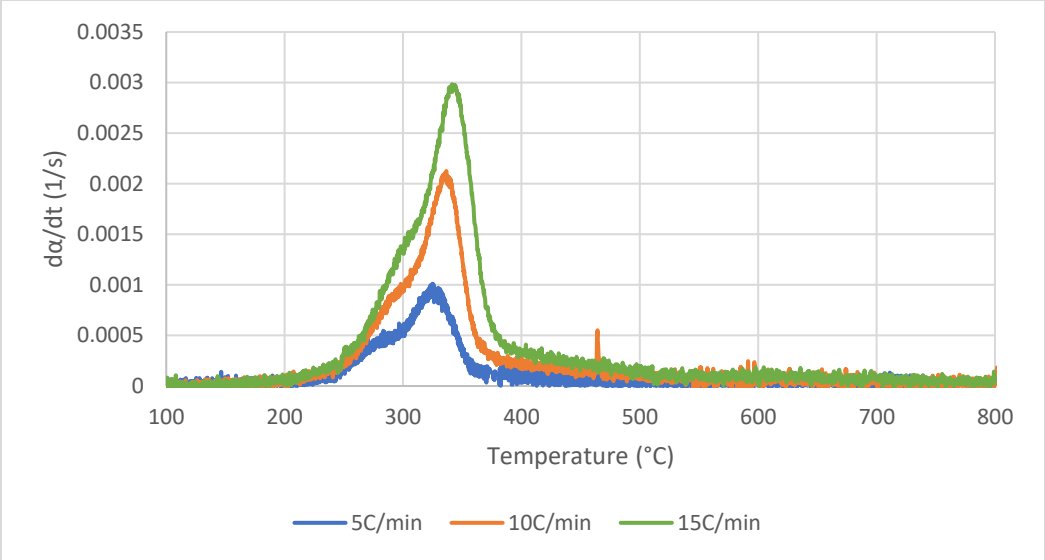

Figure 11 DTG curves for rice husk at different heat rates

4.3 Co-Pyrolysis of Chicken manure-rice husk

For the biomass blends, the TG curves for the mixtures are shown in Figure 12. For clarity, only the heat rate with the most noticeable effect (5 °C/min) is shown. However, it is worth mentioning that all the heating rates had the same effect on biomass degradation and the final residuals can be found in Table 4.

When mixing the two biomasses, the first stage occurs at the temperature range 100-220°C, which corresponds to the humidity extraction. The average humidity content of the blends was 10%wt, which is approximately equal to the humidity in the individual biomasses. The second stage of decomposition occurs at the 250-360°C temperature range. In this stage, the hemicellulose and cellulose from both biomasses decompose. In addition, the decomposition of lignin slowly initiates. This stage has the most massive mass degradation with around 40%wt on average. The third stage occurs at temperatures higher than 360°C, during which the crystalline cellulose and

the more stable components in the lignin (benzenes) are slowly degraded. This stage decomposes about 20% of the total volatiles.

Figure 12 shows that the degradation follows a straight line during the 250-340°C range. To have a better understanding of the decomposition at this stage. The TG curves at this temperature range are approximated to a straight line (Figure 13). From Figure 13, it is clear that increasing the rice husk mixing ratio increases the degradation. At 250°C the lost mass is almost identical within all blends. However, when more rice husk is added, an acceleration occurs in the degradation. As such, at 340°C the degradation increased from 0.7 to 0.51 (marked in Figure 13). Despite this acceleration, the TG lines for all the blends are almost parallel in this stage – indicating that the decomposition of the different components takes place at the same temperatures, still the rice husk acts as a catalyzer. This result can be explained (1) by the similarities in the volatile matter between chicken manure and rice husk [80-81]; and (2) the silica content that may act as a catalyzer of the reaction. Further discussion of catalyzing and synergetic effects is provided in the subsequent section.

The DTG curves for the first stage of degradation remained relatively unchanged when rice husk was added (Figure 14). For the second stage, the degradation rate increases when the percentage of rice husk increases. The chicken manure's degradation rate is increased because there is additional heating provided by rice husk decomposition. However, the degradation peak is slightly delayed, causing a need for higher temperatures to reach the degradation peak (Figure 14).

Figure 15 to 18 show the comparison between measured and calculated degradation (using Equation 10) for three different blends. The model can predict the behavior of the mass conversion quite well, thus validating the equation. However, after 340°C, increasing the mixing ratio causes

a discrepancy between the predicted and experimental data. The main reason for the difference is the synergetic effects between the two biomasses. Identical behavior was found by Mallick when mixing rice husk with sawdust [57]. The total conversion of the blends was higher than the additive degradation of the individual biomass. The maximum increase in the degradation corresponds to the mix of 60%CM+40%RH. In this case, the discrepancy starts at 240°C. The predicted remaining mass using equation (10) is 36%wt, while the measured mass is 26%wt, as shown in Figure 16. Compared with the degradation of chicken manure at the same heating rate, there is an observed improvement of 47% over the overall biomass conversion, indicating that the extractives of the chicken manure are enhancing the degradation of the blend and giving higher conversions.

Table 4 shows the remaining biomass for different heating rates. The increase in the heating rate reduced the conversion percentage for all the blends except for a few cases where the remaining mass was higher than the mass of a singular biomass. In addition, increasing the heating rate decreases the synergetic effect - meaning that the calculated and the measured curves are closer to each other. This result is a consequence of fewer extractives being released when the heating rate is increased.

The effect of the synergy between the two biomasses has a significant effect in the energy of activation, which is discussed in the next sections.

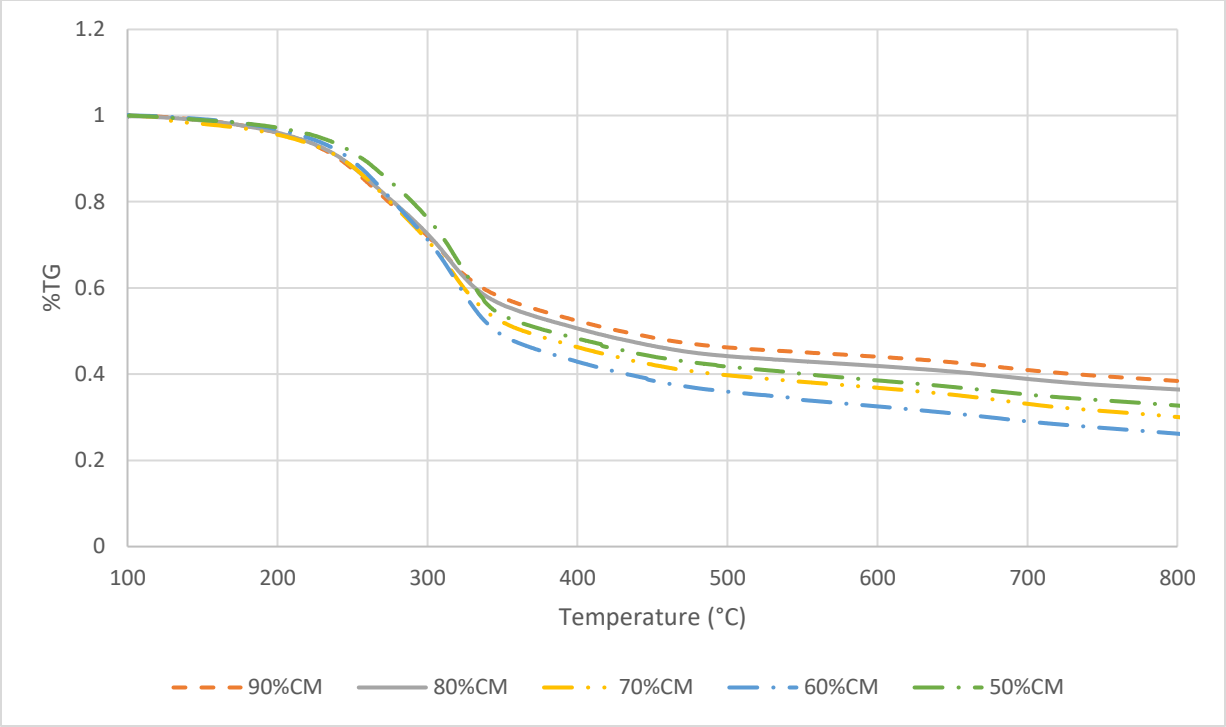

Figure 12 TG curves for different mixing ratios at 5 °C/min

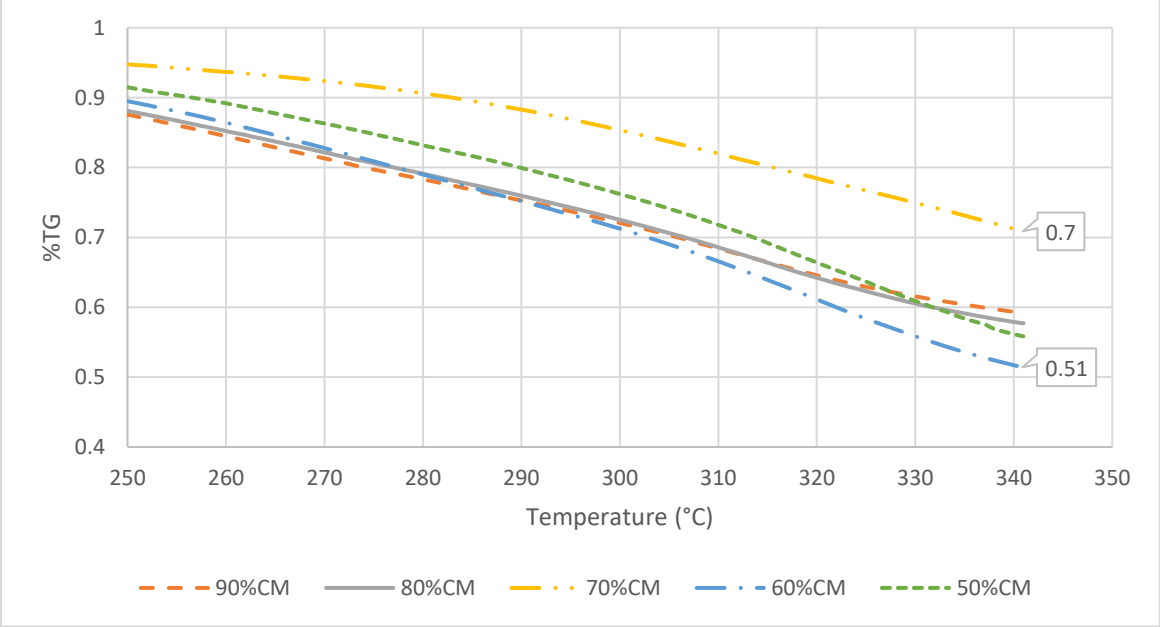

Figure 13 TG curves between 250°C and 340°C at 5 °C/min

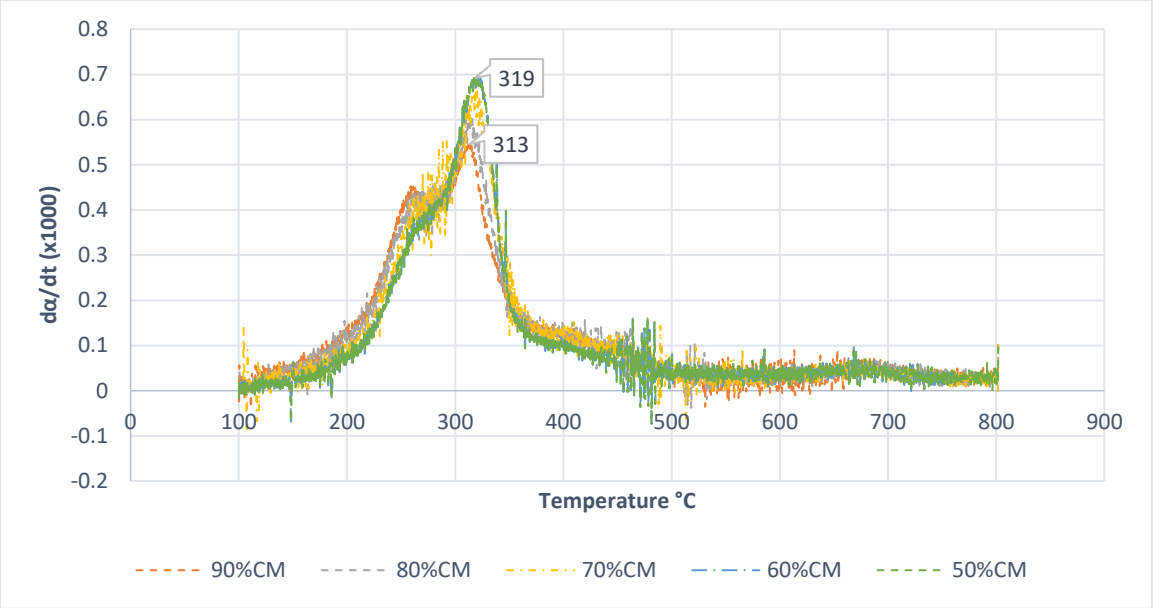

Figure 14 DTG curves for different blends

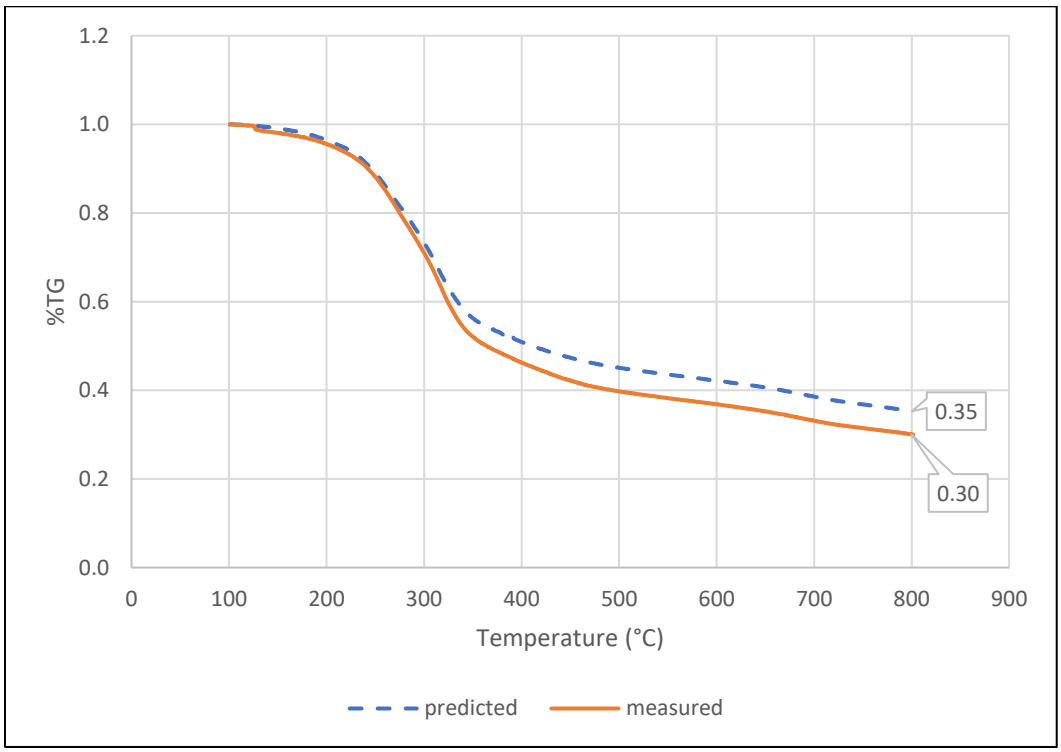

Figure 15 TG curve for 70%CM+30%RH

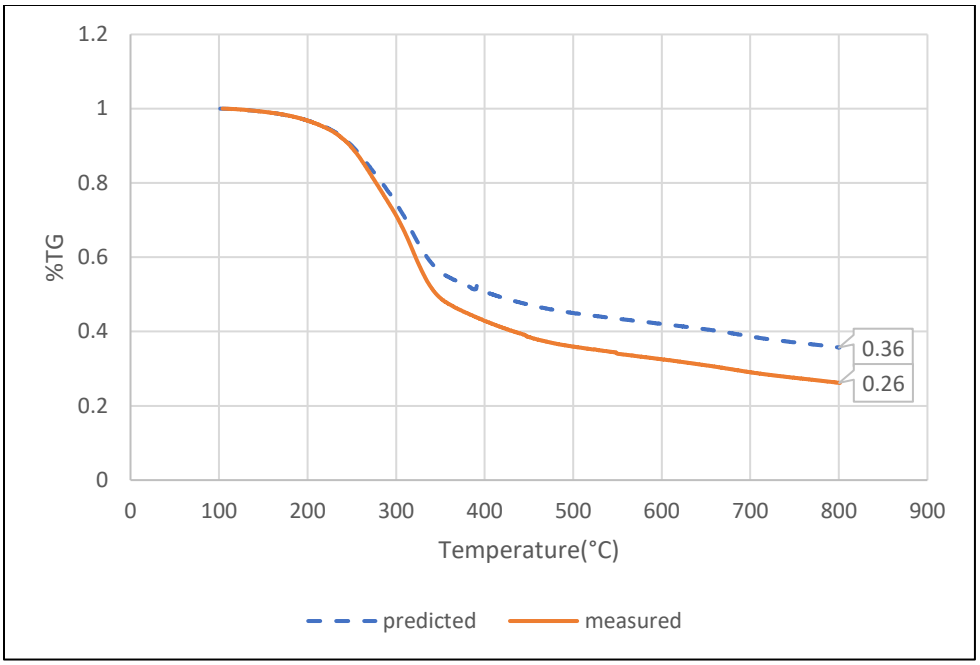

Figure 16 TG curves for 60%CM+40%RH

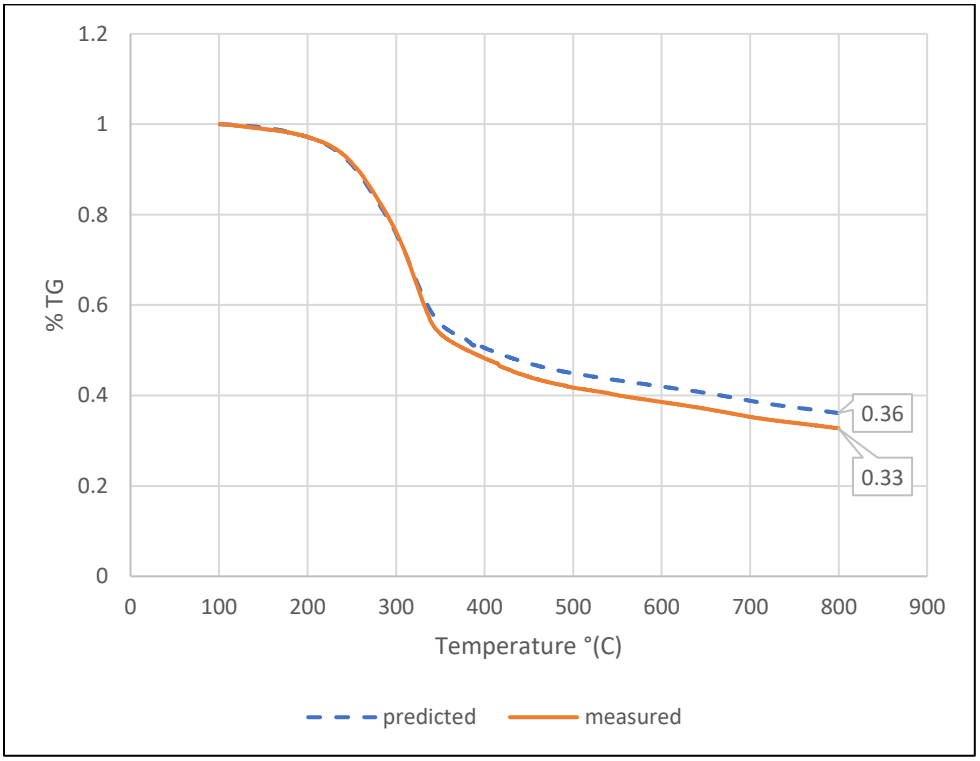

Figure 17 TG curves for 50%CM+50%RH

Table 4 Biochar percentage for different heating rates and mix ratios

%CM	%Biochar		
	5°C/min	10°C/min	15°C/min
100	34	36	36
90	39	34	41
80	37	34	35
70	30	34	33
60	26	36	34
50	33	31	34

4.4 Nitrogen Pyrolysis DTA analysis

The differential thermal a nalysis curves for different mixing ratios are shown in Figure 18. To illustrate the evaporation process, the DTA curves go from ambient temperature to 800°C.

The curves are consistent with the DTG curves, the maximum degradation rate, and the peaks in the thermal energy, which all occur at the same temperature. Four peaks are characteristic in all types of the studied pyrolysis. Increasing the heating rate increases the magnitude of the peaks and delays the temperature at which these peaks occur. Even though it is observed that the general trend is followed for all the heating rates, at low heating rates, the energy extracted from the different blends is almost identical. However, higher variations in the DTA curves are observed for higher heating rates. The general trends are described below.

The first portion represents the water evaporation. During water evaporation, initially, the reaction is highly endothermic up to temperatures of 100°C. Then the evaporation continues up to temperatures of 120°C. The degradation of hemicellulose and cellulose peaks at a temperature of about 350°C. This stage is characterized by different reactions that compete simultaneously. Such reactions tend to be exothermic for lignin and hemicellulose. However, for cellulose, the dominant mechanism depends on the biomass and heating rate. The exothermic behavior of the DTA implies that the exothermic mechanisms are dominant for this stage of pyrolysis. The energy extracted remains stable up to 380°C.

Combining the two samples increases the amount of energy released during the reaction. When comparing the energy released, each biomass sample stood alone because each biomass provides a similar exothermic reaction over the same temperature range. At the early stages of pyrolysis, chicken manure has the least energy extraction mainly because all the energy supplied by the furnace is being used to remove moisture content. Also, the hemicellulose decomposition is less exothermic than the decomposition of other constituents. However, for 0% chicken manure (100% rice husk), it can be observed that the existing energy is higher due to lesser moisture content, the absence of hemicellulose, and an exothermic reaction of cellulose (presumably char formation). By adding more rice husk (10% and 20%), the DTA curve is then located between 0% and 100% chicken manure, which emphasizes this conclusion. When more rice husk is added, the exothermic reaction is dominant.

When moving onto analyzing to the middle zone, starting from 260 ^{o}C (which corresponds to thermal degradation of hemicellulose in chicken manure) to 480 ^{o}C (where only lignin is degraded), it is observed that the amount of energy released from the reaction for all mixture blends

is higher than that of each sample alone. The main reason behind this result is the overlap between two exothermic reactions taking place at the same time.

For the secondary pyrolysis (after 500°C), the endothermic reactions (such as water-gas reaction) from cellulose and lignin become more dominant than the exothermic reactions, thus explaining the fast drop in the energy extracted. For chicken manure, the temperature at which the reaction becomes fully endothermic varies between 600 and 770°C. For rice husk, such temperature varies between 630 and 690°C. Adding rice husk causes a delay in this temperature reaching a complete endothermic resolution, signifiying a more self-sustaining pyrolysis. Among all cases, the case 60% chicken manure mixture gives the highest exothermic reaction.

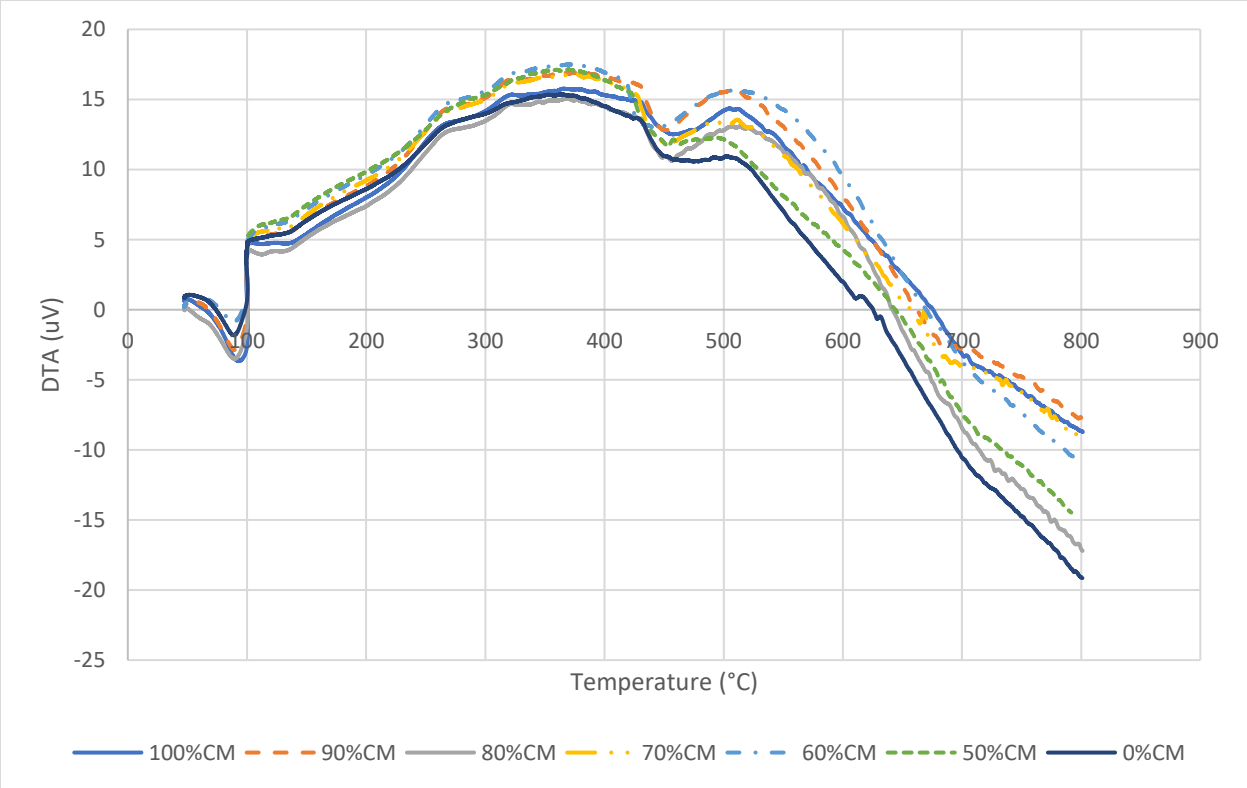

Figure 18 DTA for different blends at 5°C/min

4.5 Kinetics of Nitrogen pyrolysis

The kinetic parameters for the reaction between 250°C and 360 °C and from 360°C to 600°C were calculated for each blend at different heating rates. The average values for each combination are shown in Table 5. For the second stage, the average energy of activation of chicken manure and rice husk is 108.1 Kj mol^{-1} and 95.5 kJ mol^{-1}, respectively. While, for the third stage, the average energy of activation for chicken manure and rice husk is 67.1 kJ mol^{-1} an d 51.9 kJ mol^{-1}.The pre-exponential factor was found to remain constant with temperature. For chicken manure and rice husk the frequency factor is $2.05 \times 10^{10} min^{-1}$ 1.17×10^{8} min^{-1}, respectively. For both types of biomass, the kinetic parameters are relatively close to the parameters obtained in literature [17-60] and Ahiduzzaman [53]. The order of reaction of rice husk was 2.0, while the order of reaction for chicken manure was 5.0. For the blends, the order of the reaction was found to vary linearly with the blend ratio.

The reason for higher energies of activation for the second stage and much lower energies for the third stage is because of the nature of the reaction. The decomposition of cellulose, hemicellulose, and lignin starts breaking down the highly polymerized components into smaller molecules (such as cellulose creating levoglucosan). This process requires significant amounts of energy to start the reaction. On the other hand, the third stage also uses the already decomposed hemicellulose, cellulose, and part of the lignin to produce syngas.

The addition of rice husk increased the energy of activation compared with individual types of biomass for the first two mixing ratios. This increase could be due to the difference in particle sizes and shape of rice husk compared to chicken manure. That size difference negatively affects the pyrolysis reactions due to the temperature gradients, also leading to lower conversion.

However, after adding more than 20% RH , the energy of activation and pre-exponential factor starts decreasing.

The minimum energy of activation for the second stage is 95.0 kJ mol^{-1} for the blend (60%CM+40%RH). This minimum value signifies a decrease of 12.1% of the energy of activation when compared with chicken manure's energy of activation. For the third stage, the minimum is 56.8 kJ mol^{-1} for the blend (70%CM+30%RH) .This decrease in the energy of activation means that the synergetic effects overcome the heat and mass transfer effects of the mixture (Table 5). One plausible reason for this result is the silica present in the ash of rice husk can acts as a catalyzer, facilitating the pyrolysis. The comparable behavior was observed in literature [60] for the gasification of chicken manure and rice husk under a fluidized bed.

Experiments show that the increase in the heating rate, in turn, increases the energy of activation of pyrolysis because less time is given before the temperature increases. As a consequence, the reactions in the pyrolysis cannot be completed, increasing the energy of activation (Figure 19-Figure 20). Also, the pyrolytic reactions cannot be perfected or reach an idyllic level of completion because less time is given before the temperature decreases, thus increasing the energy of activation.

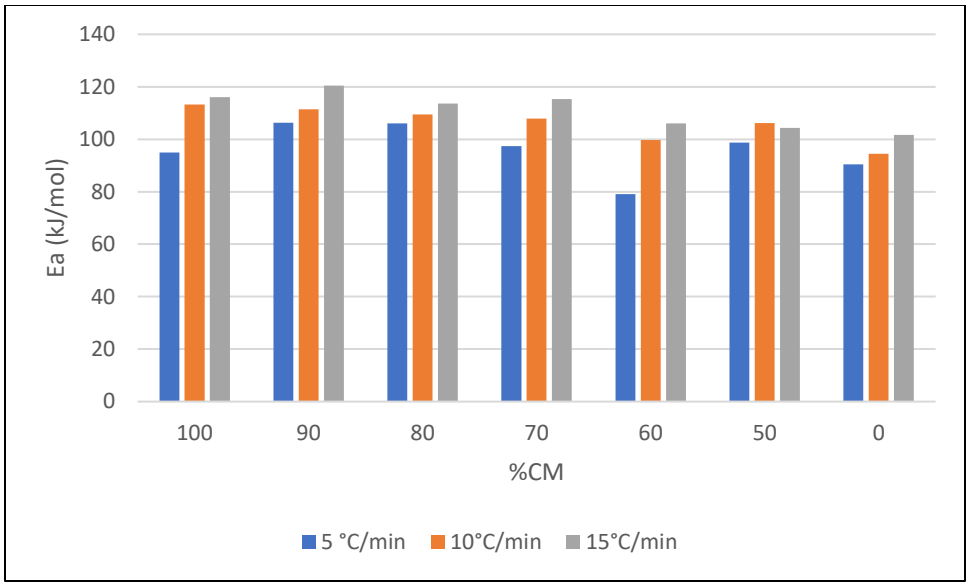

Figure 19 Energy of activation for different cases at 2nd stage

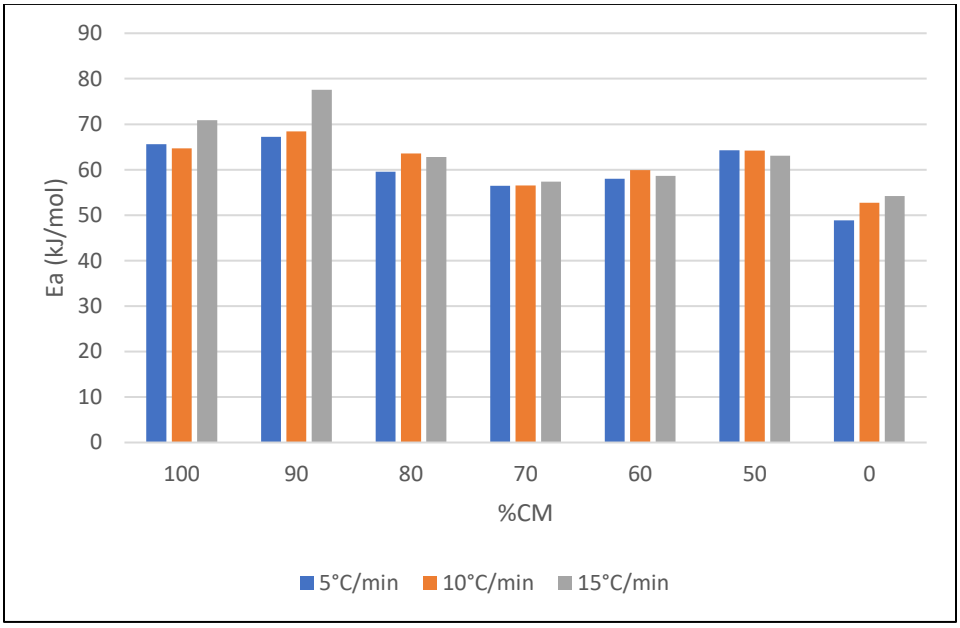

Figure 20 Energy of activation for different heat rates 3rd stage

Table 5 Averaged Kinetic parameters

%CM	n	Ea (kJ/mol)	A (min-1)
100 (250-360°C)	5	107.0	1.7E+10
100(>360°C)	5	67.1	1.7E+10
90 (250-360°C)	4.7	112.7	2.4E+10

90(>360°C)	4.7	71.1	2.4E+10
80(250-360°C)	4.4	109.7	5.4E+09
80(>360°C)	4.4	62.0	5.4E+09
70(250-360°C)	4.1	106.8	3.8E+09
70(>360°C)	4.1	56.8	3.8E+09
60(250-360°C)	3.8	95.0	5.9E+08
60(>360°C)	3.8	58.9	5.9E+08
50(250-360°C)	3.5	103.1	7.3E+08
50(>360°C)	3.5	63.8	7.3E+08
0(250-360°C)	2	95.5	1.2E+08
0(>360°C)	2	52.0	1.2E+08

4.6 Air gasification of chicken manure

When air is used as a reacting atmosphere, gasification is expected due to the partial oxidation of the biomass (at low equivalence ratio). To ensure partial oxidation, the flow rate of air was set to 5 ml min^{-1} and the flow rate of nitrogen at 100 ml min^{-1}, which signifies an equivalency ratio of approximately 0.23. Chicken manure air gasification can be divided in four main steps (Figure 21). Similarly, to chicken manure's pyrolysis, the first step is drying. During this step, approximately 10% of the total mass was removed as moisture.

The second step is the pyrolytic stage, where hemicellulose and cellulose are decomposed. This stage starts at temperatures between 200-350°C. This step has a significant mass loss. The DTG curves exhibit two degradation peaks at 257 and 300°C (Figure 22). These peaks correspond to the degradation of hemicellulose and cellulose. When comparing with the nitrogen case, it is observed that the presence of oxygen seems not to affect temperatures where the peaks of degradation occur. However, the magnitude of the degradation peaks is slightly larger than the peaks' magnitude for chicken manure pyrolysis. It is also observed that the magnitude of the first peak (hemicellulose degradation) is more significant than the magnitude of the second peak - signifying that the degradation of hemicellulose occurs faster. A plausible reason for that result is

the presence of oxygen that promotes reactions that generate CO2 and CO, further accelerating the decomposition of hemicellulose. For the case of cellulose, due to the low content of C=O bonds, the release of CO2 is much smaller, then the presence of oxygen will not affect the degradation peak of cellulose.

Subsequently, the third step happens at temperatures between 350 and 450°C. This step occurs at a slower and relatively constant rate when compared to the second step. The third step corresponds to the degradation of the crystalline part of cellulose and degradation of the benzenes present in lignin. This stage shows a steady degradation rate that corresponds to the decomposition of the more stable components (crystalline cellulose and lignin). Similar to previous cases, increasing the heating rate increases the decomposition rate but decreases conversion.

At the 450- 520°C temperature range a significant and quick mass loss occurs. The rapid degradation rate at a short period of time indicates that the sample is igniting. This step has one peak of degradation and two smaller shoulders (Figure 22). The shoulder-like shapes can be explained because the ignition is a mass transfer limited process. Thus, the mass that could not be oxidized during the first ignition peak will be oxidized at higher temperatures. That also explains why increasing the heating rate makes the reaction wider and the shoulder-like shapes more relevant.

After 600°C, no significant mass loss is recorded. However, reduction takes place after oxidation, meaning that all the products from the oxidation are reacting to create syngas through reactions such as Boudouard reactions, carbon dioxide diffusion, and water gas shift reaction. The residual mass for chicken manure was 20%, which agrees with the ash percentage given from the proximate analysis. Indicating that the remaining mass is ashes and all the organic material was fully gasified.

Similarly to the prior case of pyrolysis, increasing the heating rate increases the degradation speed and increases the temperature where the peaks occur. Also, the amount of residual mass increases when the heating rate increases. This surplus is caused by more incomplete decomposition reactions (pyrolysis, oxidation and reduction).

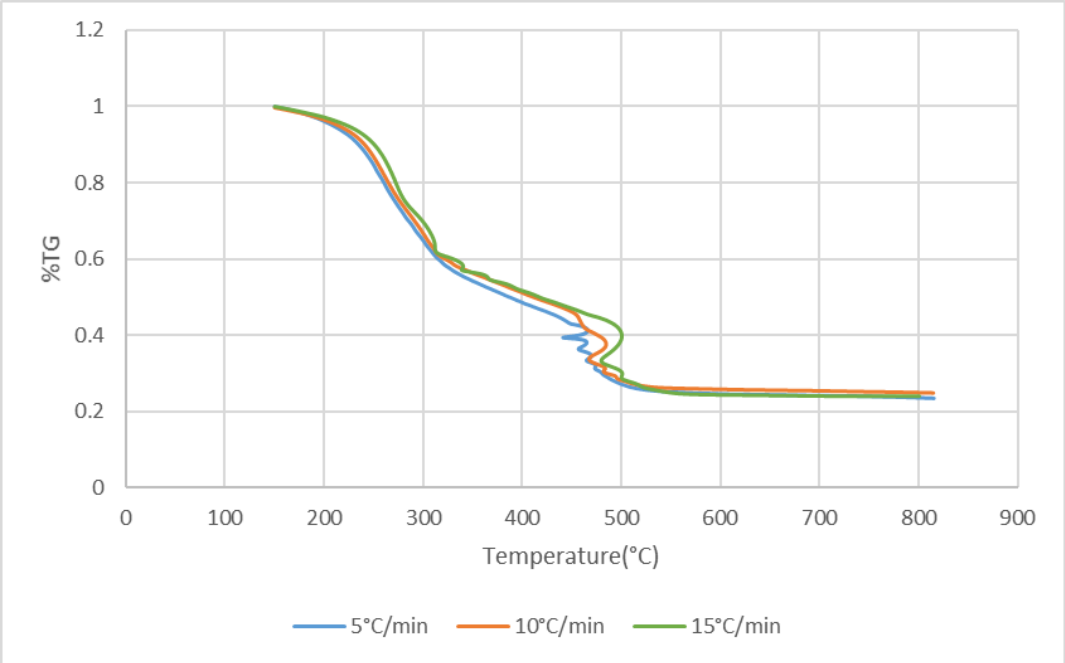

Figure 21 TG curves for chicken manure air gasification

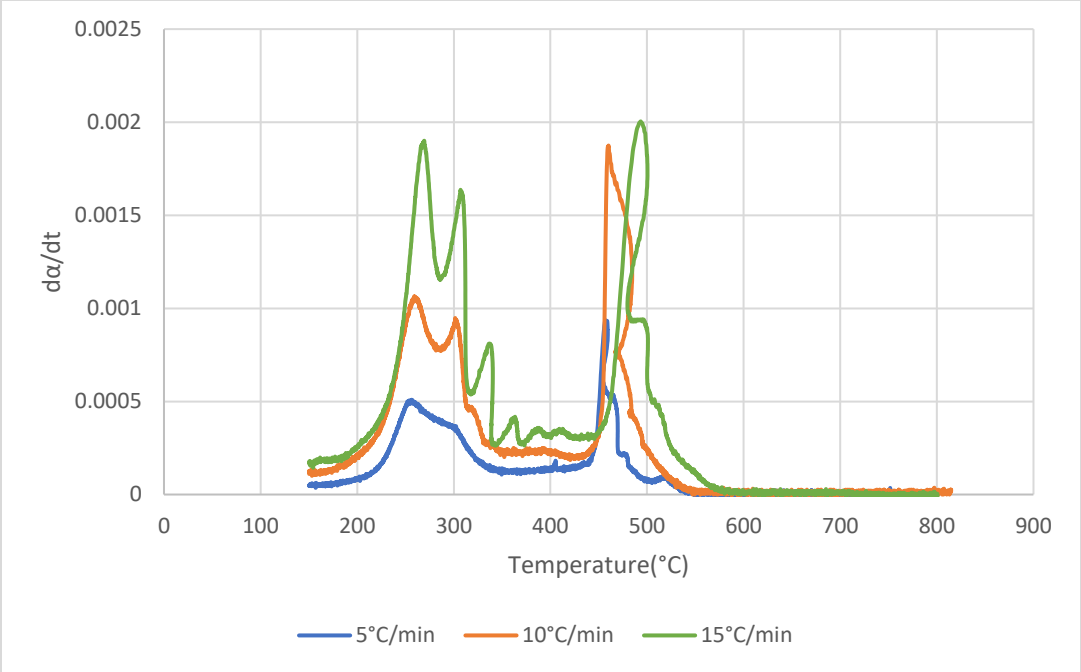

Figure 22 DTG curves for chicken manure air gasification

4.7 Air gasification of rice husk

Rice husk TG curves can be seen in Figure 23. The degradation follows four main steps: drying, thermal cracking, oxidation, and reduction. Similarly to the previous cases, drying takes place at temperatures up to 150°C. As expected, the drying process showed identical behavior when compared to the nitrogen case.

Subsequently, thermal cracking occurs in temperatures from 220-350°C. This process showed a significant mass loss, and at 320°C approximately 40% of the mass is decomposed. The next stage is occurs at temperatures from 350 to 450°C - which corresponds to the ignition of the biomass. This stage decomposes approximately 35% of the biomass.

After 500°C, less than 4% of biomass is decomposed. Thus, this stage corresponds to the reduction and degradation of the remaining carbon in the biomass. The remaining mass was almost identical for the different heat rates because the mass transfer limits the ignition process of biomass.

The DTG curves for rice husk are shown in Figure 24. Two peaks are characteristic on the degradation of rice husk. The first peak represents the maximum degradation rate for the thermal cracking of cellulose and part of the lignin. This peak occurs at temperatures between 300-306°C. This result signifies that the heating rate has a low impact on the temperature where the peak occurs. However, the magnitude of the peak increases from 7.00 to 14.05 $\times 10^{-4}$ s^{-1}.

The second peak represents the ignition of the sample. The temperature lag is more significant for this process than for thermal cracking, as shown by the process occurring at temperatures 407-421°C. The magnitude of the peak varies between 3.79-7.78 $\times 10^{-4}$ s^{-1}, indicating a higher mass loss during the ignition of the sample. After ignition no significant mass degradation was recorded.

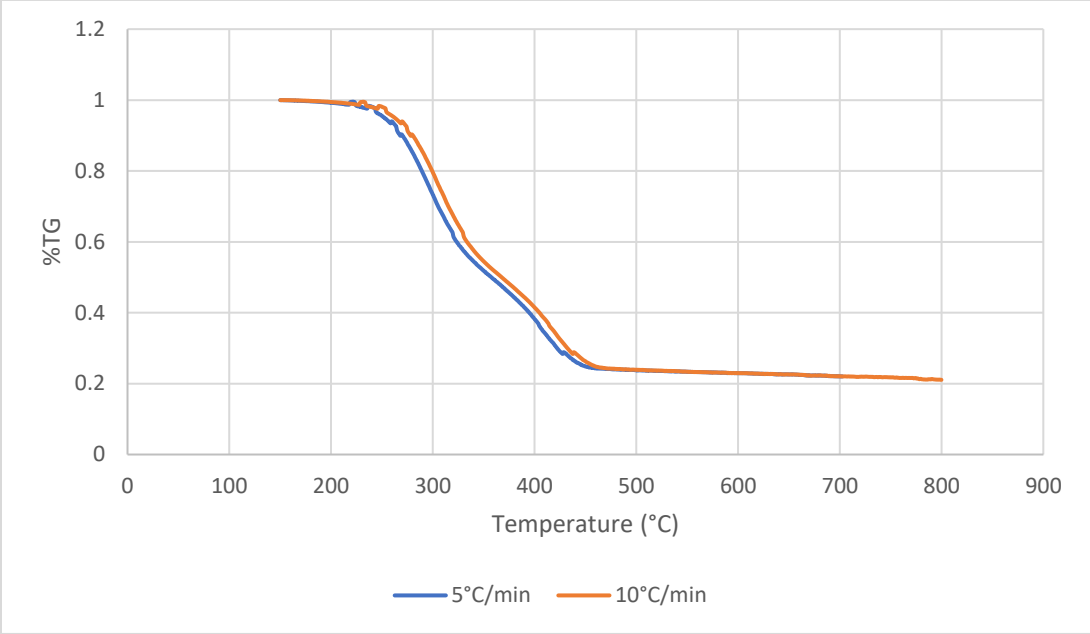

Figure 23 TG curves for rice husk gasification

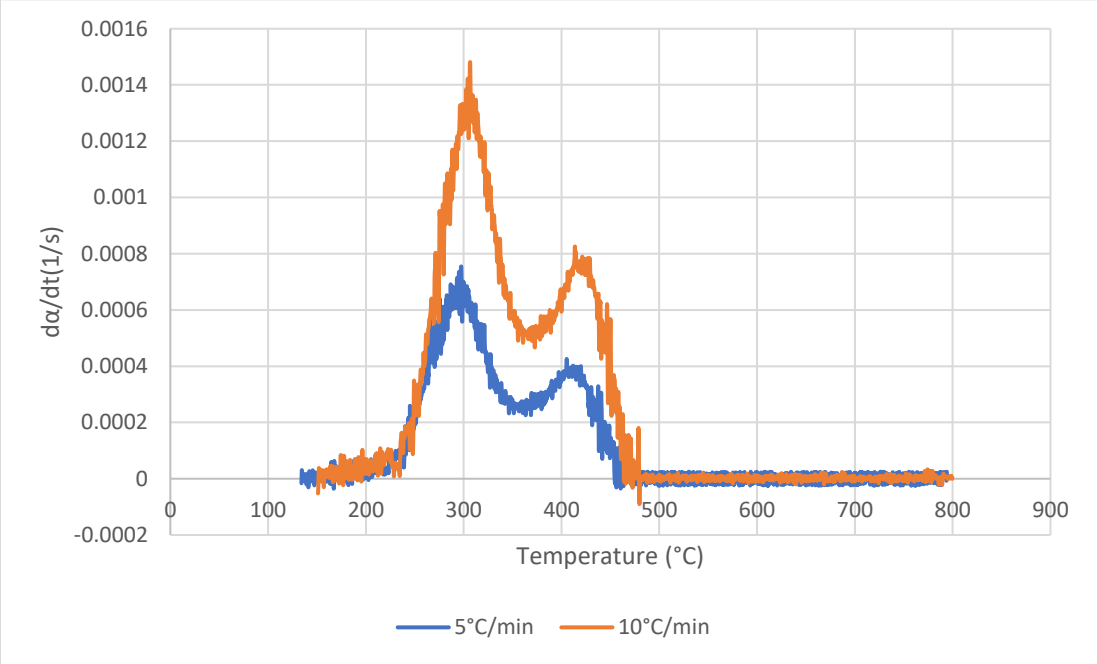

Figure 24 DTG curves for rice husk

4.8 Co-gasification of chicken manure and rice husk

The co-gasification of chicken manure and rice husk for the different blends is shown in Figure 25. The TG curves show that the co-gasification of these two biomasses can be divided in five stages: Drying, thermal cracking of light components, thermal cracking of the more stable components, ignition, and reduction.

The first stage (drying) occurs at temperatures between 100 and 220°C, which corresponds to the humidity extraction. This stage showed a mass loss of approximately 9%wt.

The second stage (thermal cracking of light components) is given at temperatures between 240°C and 320°C. In this stage, the hemicellulose and part of the cellulose from both biomasses decompose. This stage starts at intermediate temperatures between when the rice husk begins to pyrolyze and chicken manure begins to pyrolyze. Increasing the rice husk percentage showed no significant effect under the mass decomposition. This stage decomposes approximately 40% of the biomass.

The third stage (thermal cracking of the more stable components) occurs at temperatures between 320°C and 420°C. At this temperature range, the cellulose's crystalline elements and the lignin are decomposed while the ignition of rice husk occurs simultaneously. The addition of rice husk demonstrated an increase in the conversion because the ignition reactions are promoted by the rice husk. The TG curves at 420°C showed an increase in the conversion from 0.46 to 0.4 (when comparing the cases 100%CM and 50%CM).

The fourth stage (ignition) occurs between 450°C and 500°C with regards to chicken manure. This stage is the narrowest among all other stages. This stage shows a quick mass degradation, decomposing approximately 20% of the biomass. Adding Rice husk decreases the mass

decomposition for this stage, which is logical because the rice husk at this temperature range has already ignited, thus providing less mass to oxidize.

After 500°C, the fifth stage (reduction) can be observed. During this stage, there is a small conversion after oxidation is completed because the ashes from the previous ignitions burn and decompose.

The DTG curves for the different blends are shown in Figure 26. It is observed that the first and fifth stages of degradation remained relatively unchanged (for the fifth stage, the DTG lines are identical). These results are discussed in the following paragraphs.

During the second stage, adding rice husk increases the decomposition rate and makes the second peak more significant. For the blend 50% CM, the magnitude of the second peak is higher than the magnitude of the first peak. This can be explained due to the higher cellulose content in the rice husk and the additional heat provided by the hemicellulose decomposition in chicken manure that accelerates subsequent reactions.

For the third stage (320-420°C), the degradation rate increases when the percentage of rice husk increases. The DTG curves are parallel and proportional to the content of rice husk. A plausible explanation for this result is that rice husk is igniting at this temperature, providing additional heat, and quickly decomposing the rice husk.

The fourth stage shows the opposite behavior to the third stage. In the fourth stage, adding rice husk showed negative effects under the mass decomposition, decreasing the mass degradation. This result is a consequence of the previous ignition of the rice husk, the products of which (such as water vapor and CO2) slow the reactions that ignite chicken manure. Therefore, more incomplete oxidation is achieved when more rice husk is added. (Figure 26).

Figure 27 to 31 show the comparison between measured and calculated degradation for three different blends (same blends as the ones shown in pyrolysis case) using equation 10. The measured and calculated curves (using equation 10) curves are in good agreement, validating the equation for the gasification case. However, after 380°C, a disparity between the predicted and experimental data is caused when the mixing ratio is increased due to the additional heat that the ignition of rice husk is providing. In the studied cases, the total conversion of the blends was higher than the additive degradation of the individual biomass. For the case 70%CM+30%RH, the discrepancy initiates at approximately 320°C. However, such discrepancy remains constant up to 380°C (as shown in Figure 27). Compared with the degradation of chicken manure at the same heating rate, there is an observed improvement of 22% over the overall biomass conversion. There are different reasons for this result: (1) at early stages the extractives from rice husk enhance the degradation of chicken manure; (2) the ignition of rice husk gives additional heat to the reaction, facilitating the subsequent reactions; (3) Rice husk ashes are high in silica – a proven catalyzer for gasification reactions.

Table 6, shows the remaining biomass for the other studied cases. For clarity only three blends are shown. Nonetheless, all the curves follow the same behavior. The maximum increase in the degradation corresponds to the blend 90%CM+10%RH. The predicted remaining mass using eq (8) is 23%wt, while the measured mass is 17.9%wt. It is observed that the addition of rice husk in proportions greater than 10% decrease the difference between the predicted and measured remaining biomass.

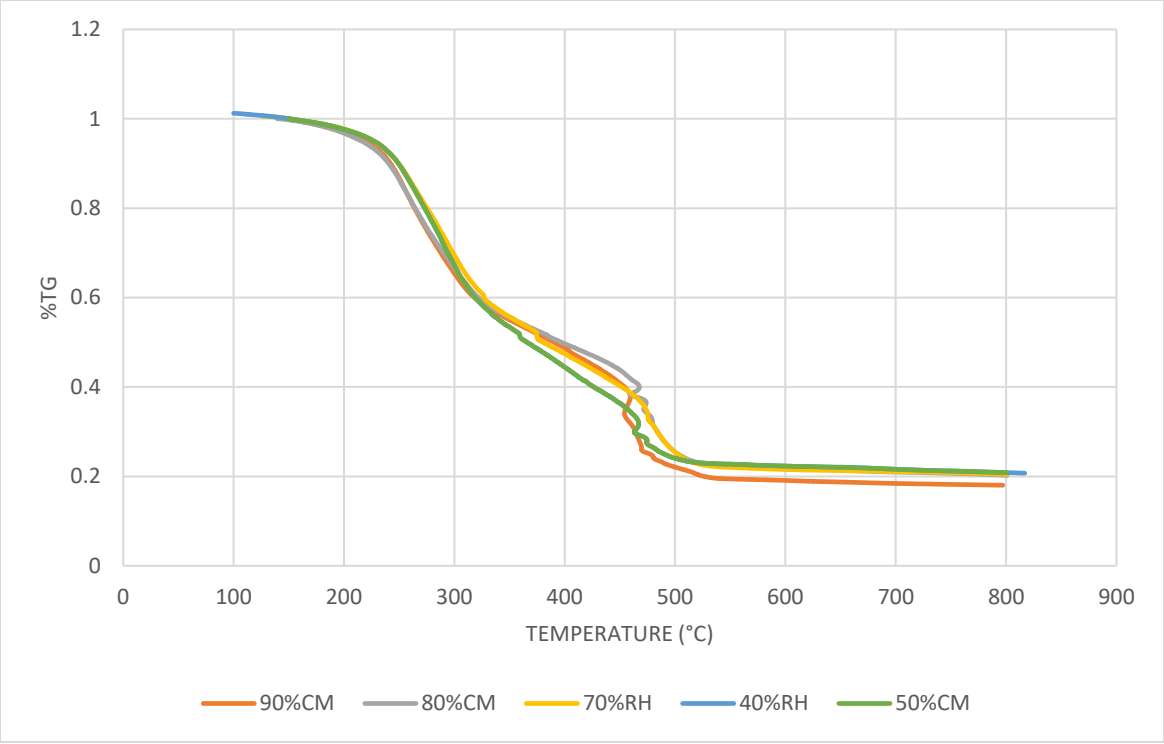

Figure 25 TG curves for gasification of different blends

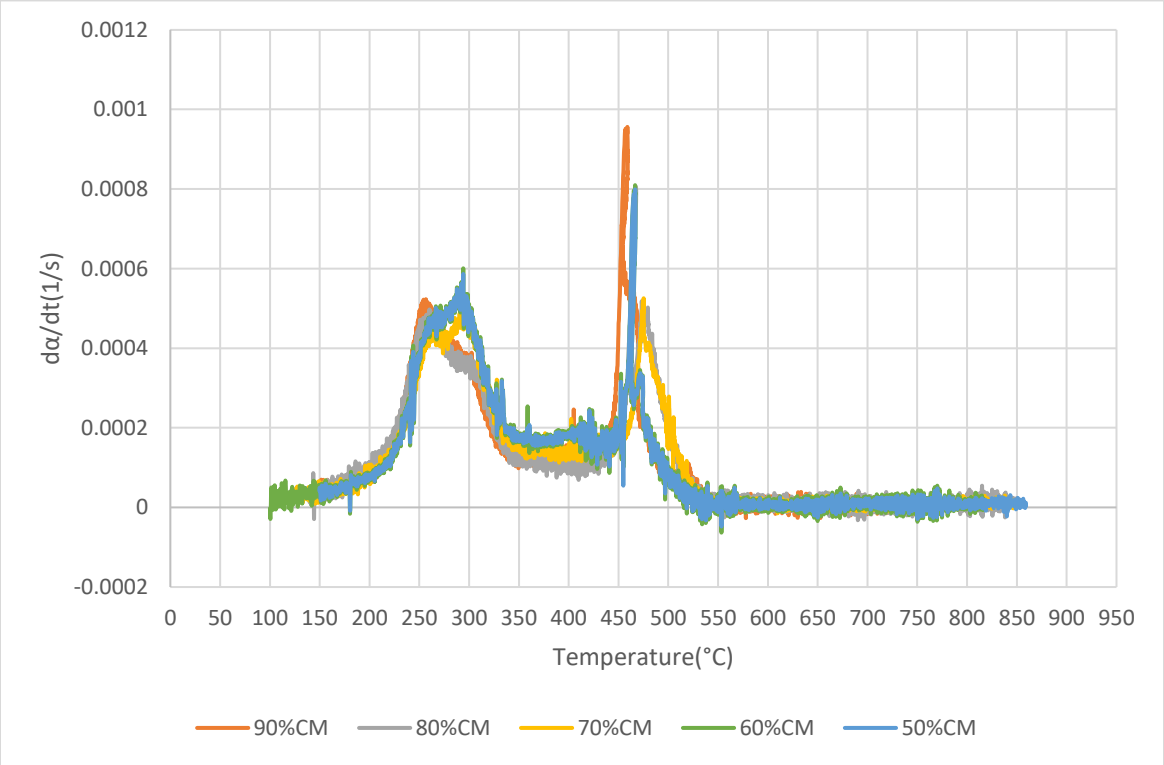

Figure 26 DTG curves for gasification of different blends

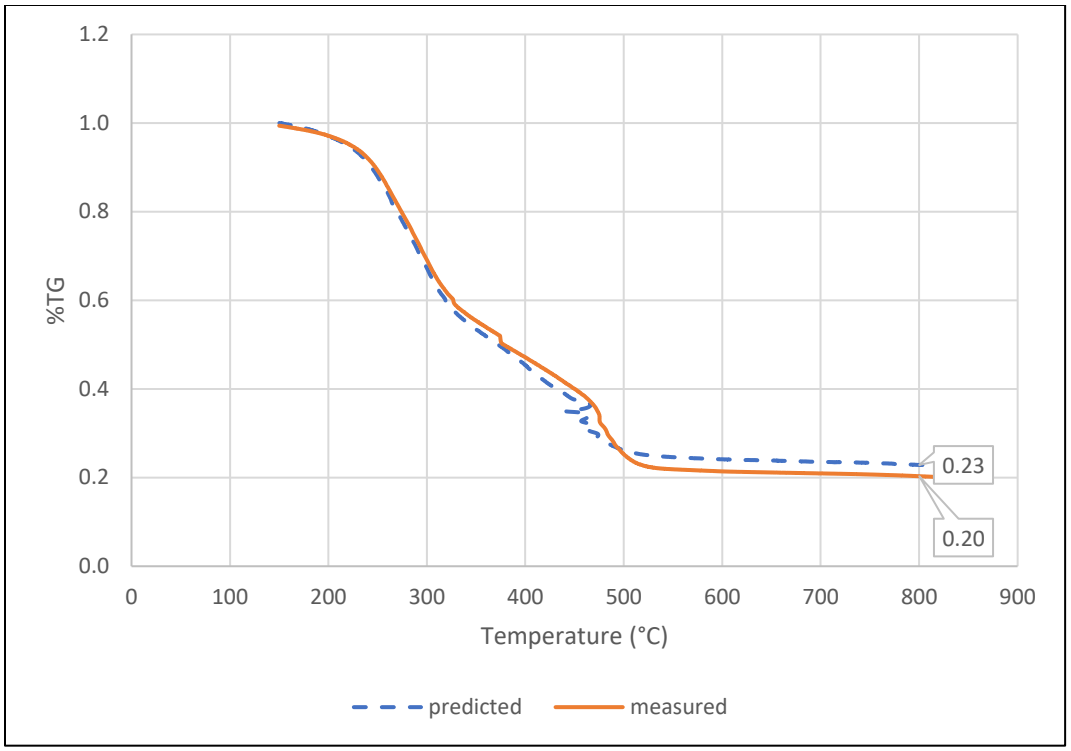

Figure 27 TG curves for 70%CM

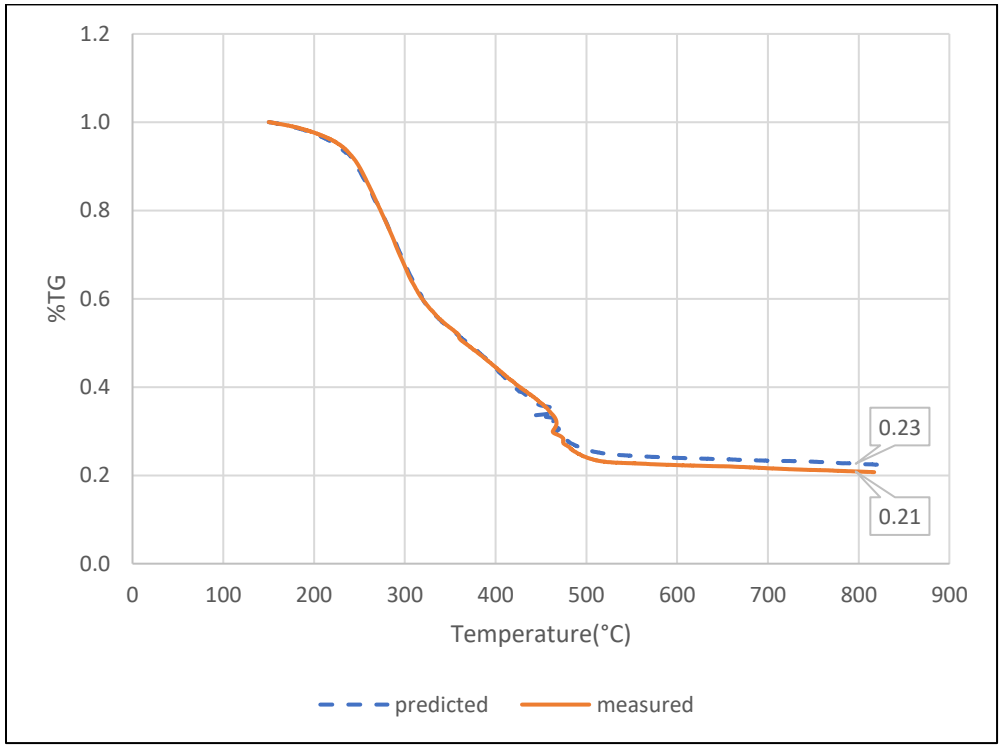

Figure 28 TG curves for 60%CM

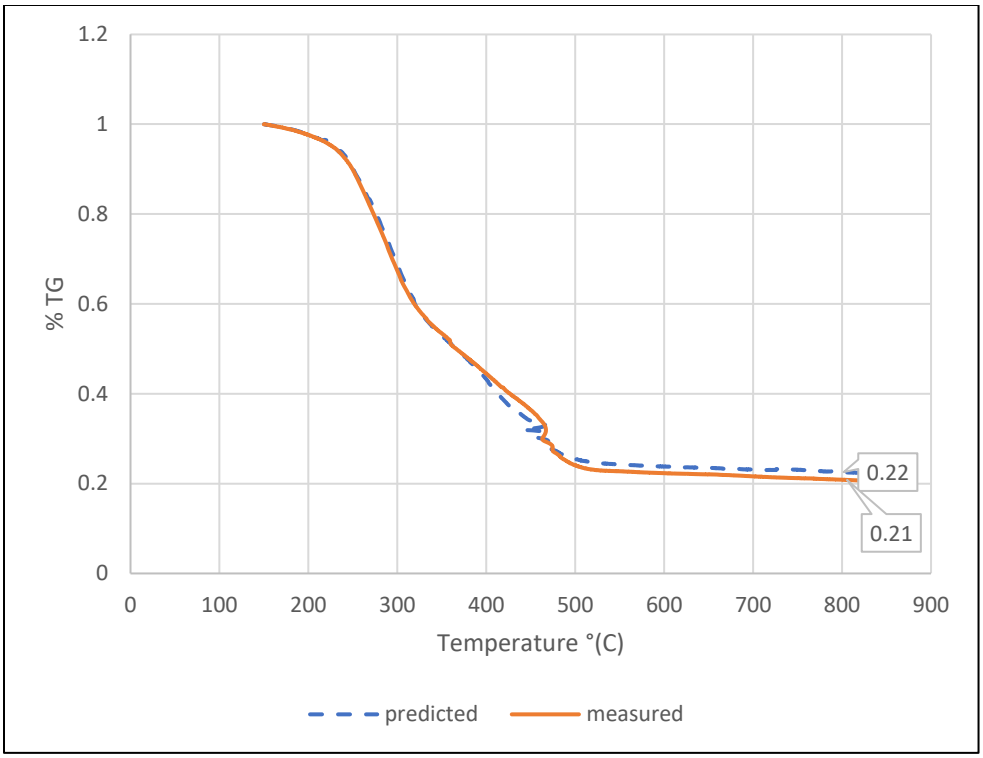

Figure 29 TG curves for 50%CM

Table 6 Residual mass for different blends

%CM	Predicted residual (%)	Measured residual (%)
100	23.4	23.4
90	23.3	17.9
80	22.9	20.2
70	22.8	20.3
60	22.6	20.8
50	22.4	20.8
0	20.0	20.0

4.9 Air Gasification DTA Analysis

The DTA curves for the gasification case is shown in Figure 30, these curves are consistent with the DTG curves. The DTA curves exhibit four peaks can be observed.

The first endothermic peak corresponds to the moisture removal. This stage goes from ambient temperature to approximately 200°C. The magnitude of the peaks is smaller compared to the other peaks in the curve, signifying that minimum energy is required to dry the samples.

The second peak corresponds to the volatilization of chicken manure and rice husk. This stage shows an exothermal behavior for all the biomasses. In the volatilization process, primary pyrolysis occurs. The exothermic behavior of this stage implies that the dominant degradation mechanism is the char formation. As such, high concentrations of CO2, CO and CH4 are expected at this temperature range. Adding rice husk increases the magnitude of the peak because of the additional heat provided by the degradation of rice husk.

The next peak corresponds to the ignition of rice husk. This stage is from temperatures from 350°C to 470°C, with the peak of this stage being at 440°C. It can be noted that the differential temperature is almost zero for the chicken manure and slowly increases when the percentage of rice husk increases. This is a consequence of the additional energy provided by rice husk oxidation. For the blend 50%CM, the magnitude of the peak is approximately equal to the energy extracted by the ignition of the rice husk standalone. After this stage the blend 0%CM (100%RH) becomes fully endothermic, proving that the reduction process is beginning.

The fourth peak corresponds to the oxidation of chicken manure. This stage exhibits a highly exothermic peak at approximately 480°C. The temperature range of this stage is from 450°C to 500°C. There is an observed overlap between the ignition of rice husk and the ignition of chicken manure. This result signifies that there are multiple decomposition mechanisms competing with each other. The oxidation of chicken manure is fully exothermic at this temperature while the decomposition of rice husk is fully endothermic; explaining the decrease in the magnitude of the ignition peak when more rice husk is added. The decrease in the ignition

peak also represents that complete combustion was not achieved, which is beneficial for gasification.

After the ignition of the samples, the reactions become fully endothermic. At this temperature, reactions, such as water shift reaction and the Boudouard reaction, become dominant (and highly endothermic). Therefore, hydrogen and CO yields are expected for temperatures higher than 500°C. The increase of rice husk makes the reduction reactions (>520°C) less endothermic, making the reaction more self-sufficient. The less endothermic reaction can be explained to the Silica content in the rice husk that can act as a CO2 absorber[82] -the CO_2 absorption is an exothermal process.

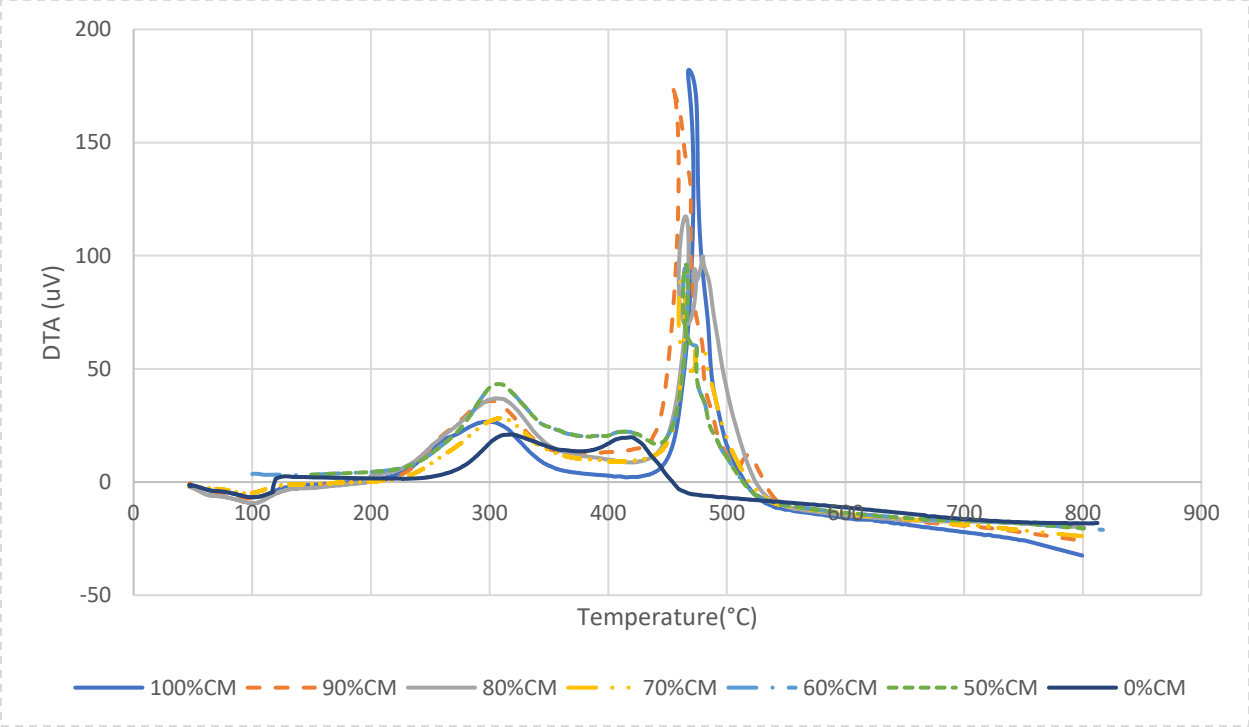

Figure 30 DTA curves for different blends at 5°C/min

4.10 Kinetics of air gasification

The kinetic parameters for air gasification are considered as a single global reaction due to the complexity of the process. The kinetic parameters are shown in Table 7 and . The Energy of activation for the individual biomasses is 72.6 kJ mol-1 and 78.5 kJ mol-1 for chicken manure and rice husk, respectively. These values are in consistent with the literature. The order of the reaction was found to be 3 for all the studied cases. This result suggests that the same decomposition mechanisms are dominant for both biomasses. The addition of rice husk decreases the overall energy of activation. The minimum energy of activation corresponded to the blend 70%CM+30%RH (63.1 kJ mol^{-1}), which means a decrease of 13% with respect of rice husk. This blend ratio value has also proven to yield the highest quality syngas for air co-gasification between these two biomasses. [60]. One plausible reason for this lower energy of activation is because the ashes from the rice husk degradation extractives (released during the char formation) have synergetic effects with the chicken manure, enhancing the decomposition. Also, rice husk biochar serves as catalyzer in the early stages, increasing the mass that is decomposed. However, when more than 30% rice husk is added to the mix, the endothermic reactions in the rice husk conflict with the reactions to decompose chicken manure. Additionally, it is harder to achieve a uniform temperature in the mixtures resulting in higher energies of activation.

Table 7 Kinetic parameters for air gasification

%CM	n	Ea (kJ/mol)	log(A/B)	A(min^{-1})
100	3.0	72.6	11.6	5.5E+05
90	3.0	70.2	13.4	3.4E+06
80	3.0	66.8	12.1	9.0E+05
70	3.0	63.1	9.3	5.2E+04
60	3.0	68.6	15.7	3.1E+07
50	3.0	81.5	14.8	1.4E+07
0	3.0	78.5	13.5	3.8E+06

5. Semi empirical model for pyrolysis products

A semiempirical model based on the previous results is developed. The model assumes that: (1) the syngas behaves as an ideal gas; (2) heat transfer and mass transfer effects are neglectable; and (3) no syngas is formed at temperatures lower than 400°C.

This model helps to determine the yields of syngas and the energy extracted from the pyrolysis. This semiempirical model is based on the work of Neves and Boateng [22,85]. The model is developed using mass balances of each component using the Equation (19) for Carbon, Hydrogen, and Oxygen respectively. The nitrogen percentage is not significant for the overall reaction. It is a common practice to combine hydrocarbons into a single component because of the lower concentrations of heavier hydrocarbons in the in the Syngas. This single component has the molecular weight of the most abundant component (in this specific case C_2H_4).

In the literature, the ratio between hydrogen and CO yields are usually estimated. The ratio is targeted to at values between 0.6-2 for the production of synthetic fuels out of the syngas [83,84]. In this study, equation 24 is obtained by correlating the experimental results from Hussein, Lima, Loy [17,86,87]. Equation 25 is developed from the model given by Neves [22]. For Biomass, the hydrogen yields are commonly described as a power or exponential function. The yield of hydrogen of chicken manure mainly depends of temperature. Equation 26 describes such dependence and the equation was obtained by correlating the experimental data from Hussein and Lima [17,72].

The energy balance uses equation 22 (for the syngas) with the heating values of H_2, CH_4, CO, C_2H_4 (see equation 27). The left-hand side of the equation describes the energy that is in the syngas. That syngas energy can be calculated as the difference between the energy in the solid fuel and the

char. In addition, the lower heating value of the gas can be estimated using equation 22 and dividing for the total mass of gas at each temperature step.

C: $$m_{cf} - m_{cch} = m_{ctar} + \frac{24}{28} mC_xH_m + \frac{12}{16} mCH_4 + \frac{12}{28} mCO + \frac{12}{44} mCO_2 \quad (21)$$

O: $$m_{Of} - m_{Och} = m_{Otar} + \frac{12}{28} mCO + \frac{12}{44} mCO_2 + \frac{16}{18} mH_{2O} \quad (22)$$

H: $$m_{Hf} - m_{Hch} = m_{Htar} + \frac{24}{28} mC_xH_m + \frac{12}{16} mCH_4 + \frac{16}{18} mH_{2O} + mH_2 \quad (23)$$

$$mCO = 13.407 mH2 + 0.0688 \quad (24)$$

$$mCH_4 = 0.146 mCO + 2.18 \times 10^{-4} \quad (25)$$

$$mH2 = 0.0038\, e^{0.0052T} \quad (26)$$

$$LHV_g(mH_2O + mtar) + LHV mC_xH_m + LHV mCH_4 + LHV mCO + LHV mH_2 = LHV_g\left(\sum_i m_{if} - m_{ch} \times \sum_i mi_{ch}\right) \quad (27)$$

Where, mcf, mof and mhf can be obtained from the elementary analysis. The heating values for each component are obtained from [88].

To calculate the masses of each element (C, H, O) in the Tar and char. Neves [22] developed the following relations that can be used to estimate the masses of each component.

$$m_{ctar} = (1.05 + 1.9 \times 10^{-4} T) \times m_{cf} \quad (28)$$

$$m_{Otar} = (0.92 - 2.2 \times 10^{-4} T) \times m_{Of} \quad (29)$$

$$m_{Htar} = (0.93 + 3.8 \times 10^{-4} T) \times m_{Hf} \quad (30)$$

$$m_{cch} = 0.93 - 0.92\, exp(-0.42 \times 10^{-2} T) \quad (31)$$

$$m_{Och} = 0.07 - 0.85\, exp(-0.48 \times 10^{-2} T) \quad (32)$$

$$m_{Hch} = -0.0041 + 0.10\, exp(-0.24 \times 10^{-2} T) \quad (33)$$

For the co-pyrolysis case, additional equations are needed to estimate the percentages of Carbon, Oxygen, and Hydrogen. In this model, catalytic and synergetic effects are neglected.

Also, the yield of biochar depends on the peak temperature in the reactor. The correlation between the biochar yield and the temperature was obtained by using the TG curves for chicken manure and rice husk. Then using equation 10 for each component gives:

$$m_{if} = (1 - f_{bm1})m_{i1} + f_{bm1}m_{i2} \quad \text{i=(C,H,O)} \tag{34}$$

$$\text{Ych} = (1 - f_{bm1})(-0.0002T + 0.3757) + f_{bm1}(-0.0003T + 0.4163) \tag{35}$$

The model was implemented in MATLAB (the script can be found in the appendix:B). The inputs of the model are the chemical composition of the raw biomass and the initial biomass temperature. The model works for temperatures between 400 and 1000°C. For temperatures lower than 400°C, the yields of valuable syngas are very low due to high concentrations of CO2 and low concentrations of other valuable gases (such as H2 or CH4) because only thermal cracking is occurring.

5.1 Model results

The predicted gas and tar yields for chicken manure and rice husk can be found in Figure 31 and 32. The values are in good agreement for the data found in the literature for chicken manure and rice husk [17,22,74,83,84]. The yields of tar decreased when temperature increased. This result is due to the thermal cracking of tar. In contrast, the yield of gas increases when the temperature increases, which could attribute to the secondary thermal cracking reactions (such as water-gas shift and Boudouard reaction). It is worth mentioning that such reactions are limited to the water and carbon oxides (CO, CO2) that are being released because in pyrolysis there is no other source of oxygen. The behavior of every gas mixture was similar. However, the yields of gas and its composition changed depending on the mixing ratio. Such change can be observed in the heating value.

The predicted syngas products can be seen Figure 33 and 35. The decay in CO2 concentration is due to the dissociation of CO_2 into CO, the Boudouard reaction (Equation 2), and the water gas shift reaction. These three reactions also explain the increases in the yields of H_2, CO. The concentration of CO_2 in chicken manure is higher than in rice husk because Hemicellulose releases more CO2 when decomposes.

For the hydrocarbons, the formation of CH_4 increases with temperature at a much smaller proportion than the other gases because the methanation reaction is not dominant at higher temperatures. For heavier hydrocarbons, the concentration increases to temperatures up to 600°C. Afterwards, the concentration of heavier hydrocarbons starts to decrease, due to the decomposition of lignin that releases heavy hydrocarbons that further break down when the temperature increases.

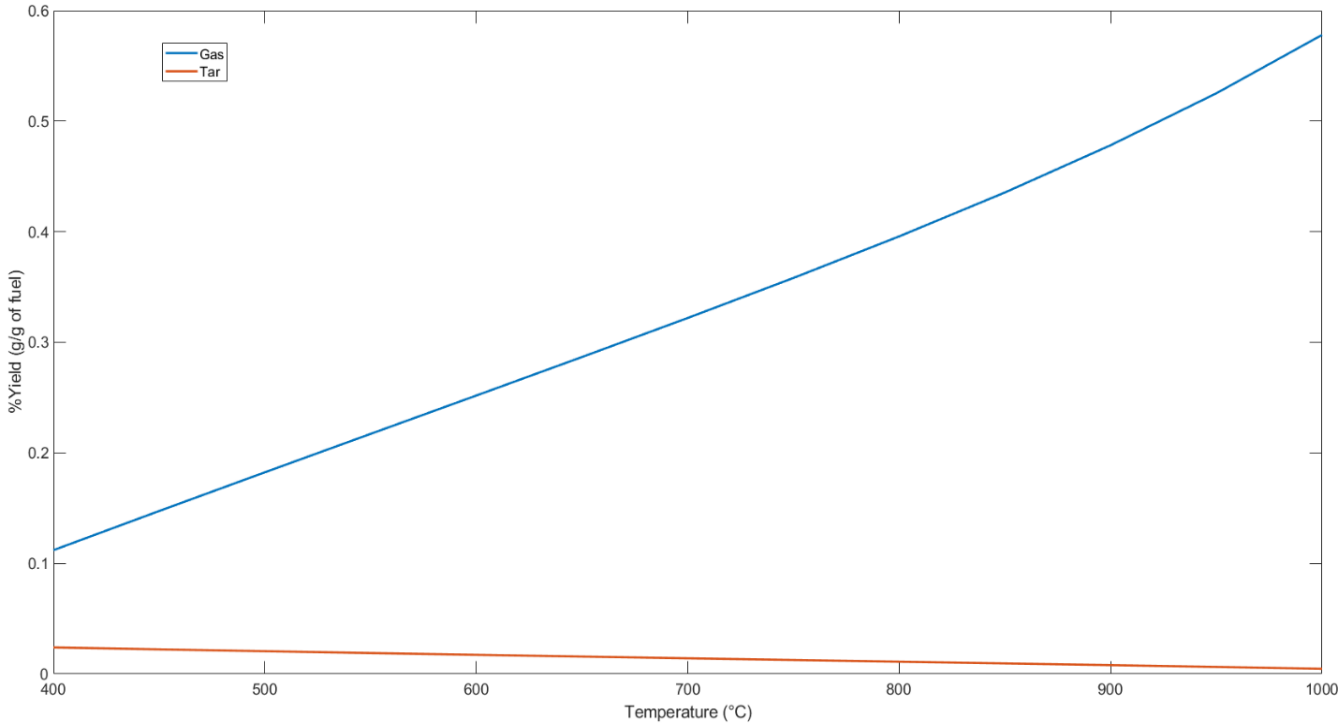

Figure 31 Gas and tar yields vs temperature case 100%CM

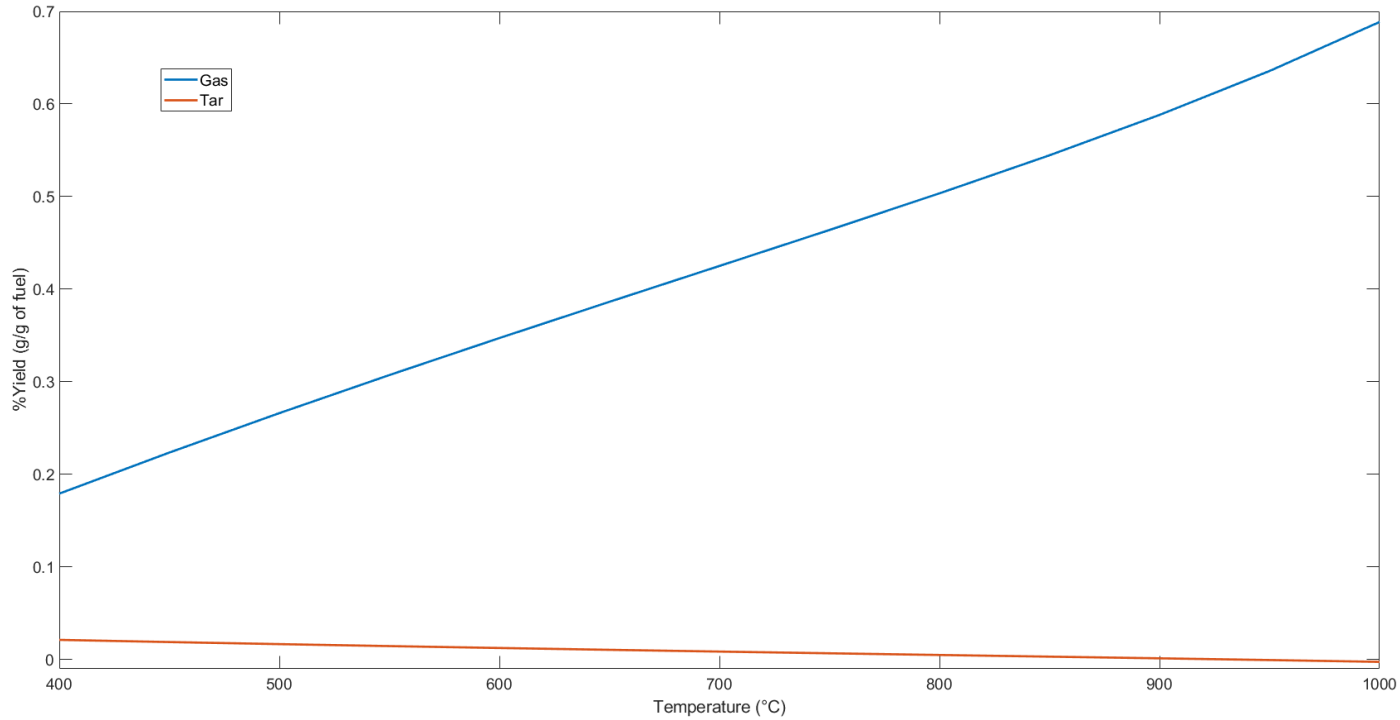

Figure 32 Gas and tar yields vs temperature case 100%RH

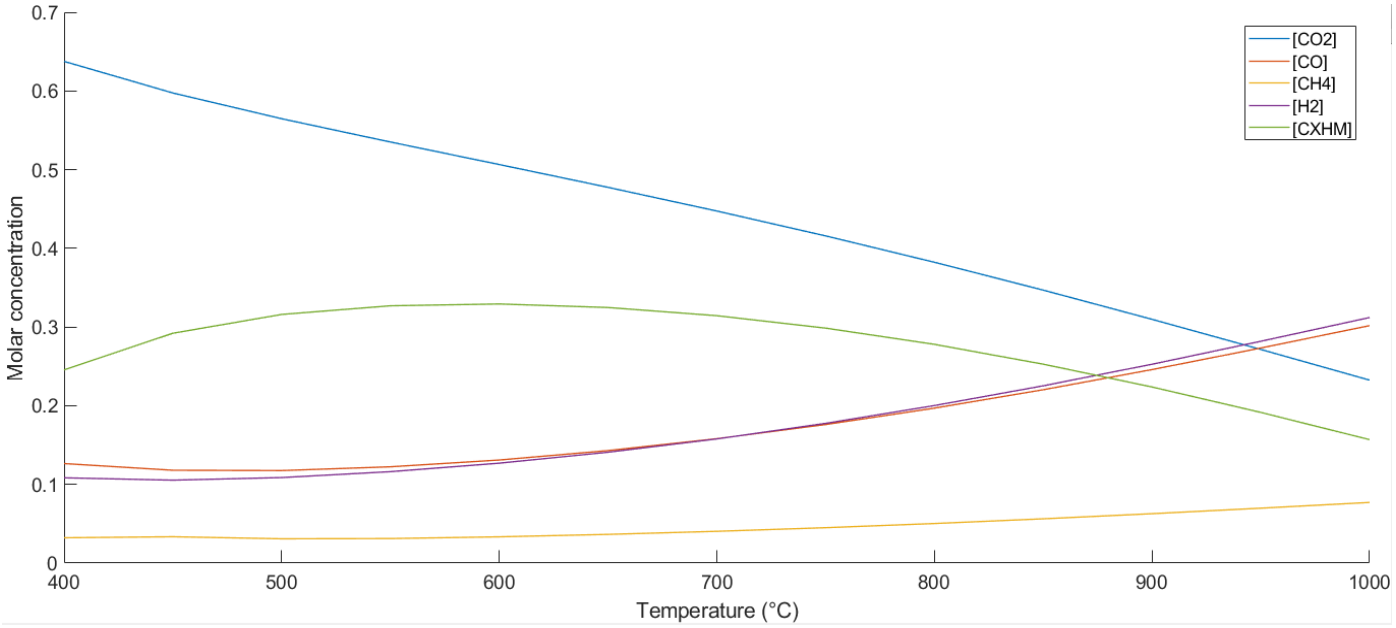

Figure 33 Syngas concentrations case 100%CM

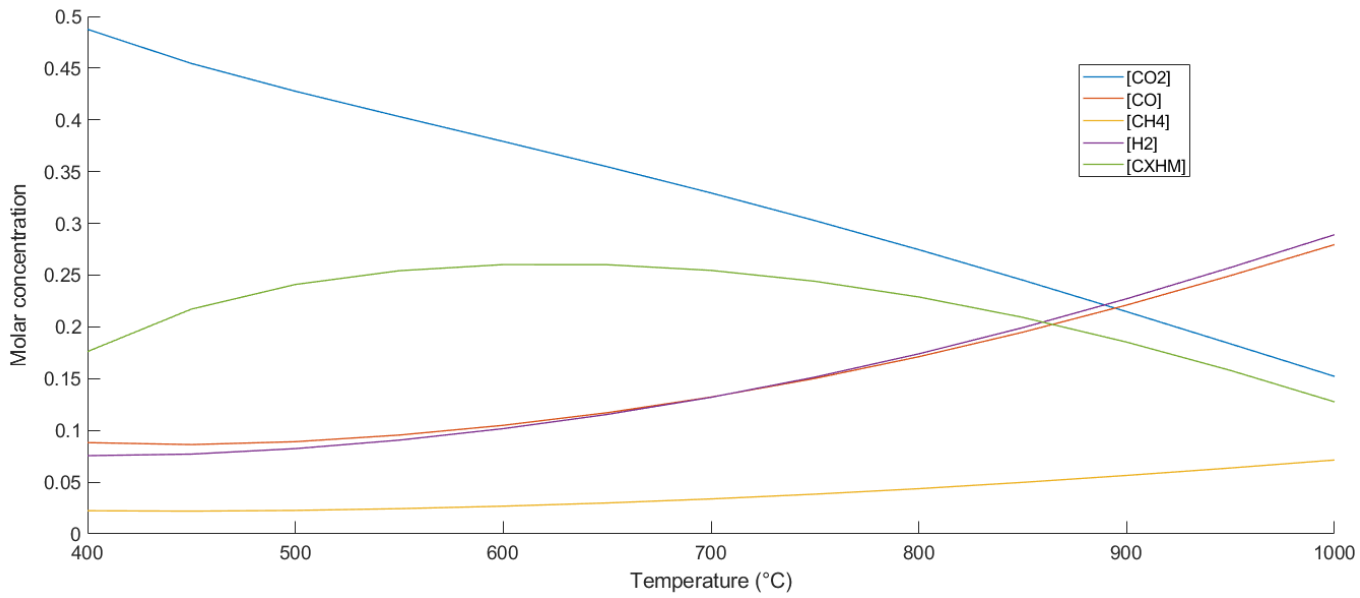

Figure 34 Syngas concentrations case 100%RH

The heating value is calculated using equation 21 for each step and blend mixture. Results are shown in Figure 35. The energy value increases with temperature, which is logical because the gas yields also increase with temperature. The highest energy value was obtained in the case of 100%CM while the lowest energy value was obtained in the case of 0%CM (100%RH). Other blends' lower heating values are between the chicken manure and the rice husk LHV curves (Figure 35). A plausible reason for this result is that the yields of CO_2 are much higher for chicken manure compared to rice husk (see Figure 33 and 34). The hemicellulose content in chicken manure produces high amount of CO_2. However, chicken manure yields slightly higher hydrogen, methane and significantly higher yields of C_xH_m, leading to higher energy value in chicken manure. In addition, synergetic effects between the two biomasses are not considered in this model, which may underestimate the heating value of the biomass mixtures. The catalytic effects can be included by adding the equations that correlate the CO_2 absorption with the silica content. Also, the synergetic effect can be added in the equation that describes the char content with temperatures.

Experimental data regarding the syngas yields must be carried on to refine the model. However, the predictions for individual biomasses and the general behaviors are accurate.

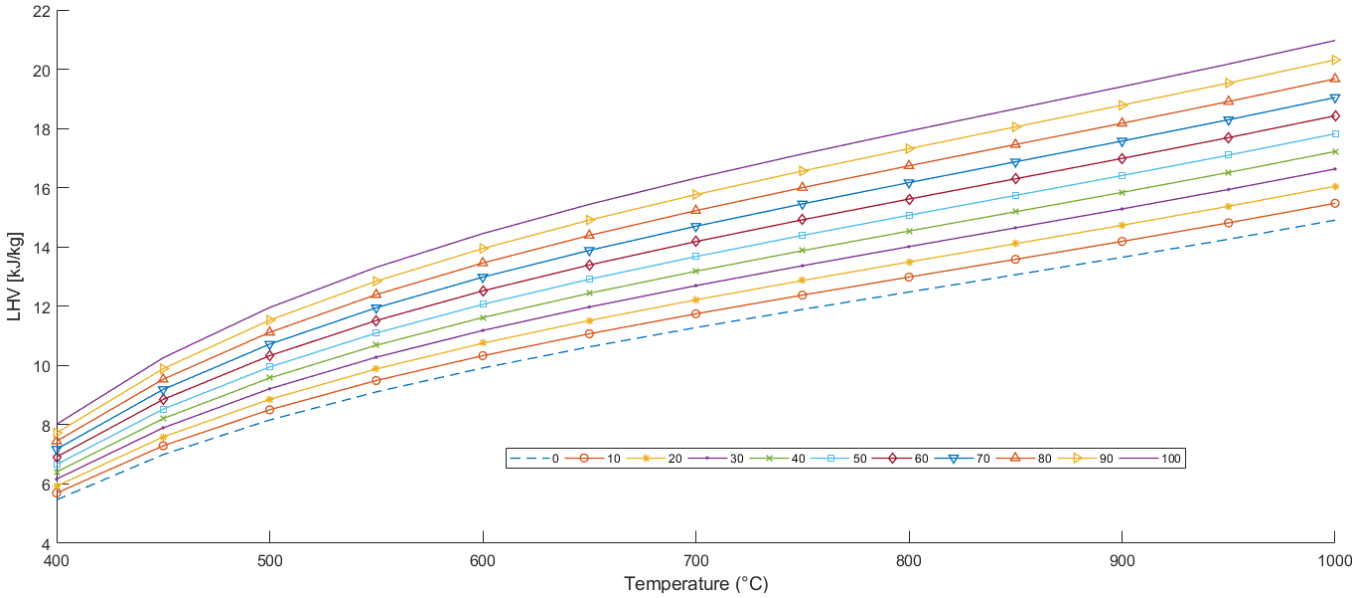

Figure 35 LHV for different blends

If the blends LHV are contrasted with the calculated kinetics, the optimal blend is 60%CM+40%RH because this mixing ratio has: (1) has the highest conversion (26% improvement); (2) the lowest energy of activation for the second stage; (3) the most self-sustainable reaction (see Figure 18); and (4) the reduction on the LHV is approximately 12% (However, it could be higher when considering the synergetic effects). These results need to be validated with experimental data.

6. Conclusions

The heat rate affects the conversion rate - the higher the heating rate is, the less time there is for reactions to complete. Also, a higher heating rate leads to a more uneven temperature distribution in the biomass particles. This result occurs when the temperature increases too quickly. These two combined effects decrease conversion and increase the energy of activation.

Rice husk is compatible with chicken manure for the studied thermochemical processes. The addition of rice husk to chicken manure causes an observable positive synergetic effect and increases the conversion of the biomass for all of the observed cases (Pyrolysis and air gasification). The effect of the rice husk synergy with chicken manure manifests in the energy of activation, which decreases when the rice husk ratio increases, thus decreasing the energy needed to begin pyrolysis.

For nitrogen pyrolysis, adding rice husk increases the degradation rate, thus reducing the time that the biomass must stay in in the reactor. This reduced time in the reactor leads to an overall decrease in the energy consumed during the process.

For nitrogen pyrolysis, the blend with the best performance was 60%CM+40%RH. This blend decreased the energy of activation by 12.1% with respect to chicken manure. Additionally, a maximum increase in the conversion of 26% was achieved when the heating rate was 5 °C/min.

The semi-empirical model predicted pyrolysis of chicken manure and rice husk would yield gases which are quite close to the experimental data. The behaviors and concentrations of the products are close to the value reported in the literature.

In the semi-empirical model, the addition of rice husk is predicted to decrease the energy value of the fuel. Nonetheless, adding rice husk proved to increase the conversion of biomass and gave

a more sustainable process. It is necessary to refine the model to account for the synergetic effects and catalytic effects. Such effects can be studied using gas analysis to give a detailed explanation of the syngas reactions taking place.

For the air gasification, increasing the addition of rice husk increases the degradation rate during the pyrolytic stage. However, for the oxidation and reduction reactions (that occur at higher temperatures), the addition of rice husk limits the degradation because rice husk ignites at lower temperatures than chicken manure, thus limiting the amount of mass that is available to be reduced.

The blend with the best performance was 70%CM+30%RH. This blend decreased the energy of activation by 13% with respect of chicken manure's energy of activation. The maximum conversion was achieved for the blend 90%CM+10%RH. Adding rice husk increases the volatile yields at an early stage, limiting the ignition of chicken manure and the reactions that form syngas.

Co-pyrolysis and Co-gasification of chicken manure and rice husk demonstrated improvements in the kinetic parameters in the thermochemical process. However, more research must be conducted in evaluating other parameters that can affect the co-pyrolysis and co-gasification between these two types of biomass, such as particle size, temperature ranges, drying time and others.

References

[1] Outlook, A.E., 2020. Energy information administration. *Department of Energy*, Washington, DC 20585, pp.1-161.

[2] Biomass explained Online, Available at https://www.eia.gov/energyexplained/biomass/

Accessed (05/01/2020)

[3] Ryu, Hae Won, Do Heui Kim, Jungho Jae, Su Shiung Lam, Eun Duck Park, and Young-Kwon Park. "Recent advances in catalytic co-pyrolysis of biomass and plastic waste for the production of petroleum-like hydrocarbons." *Bioresource Technology* (2020): 123473.

[4] Gerber, Pierre J., Henning Steinfeld, Benjamin Henderson, Anne Mottet, Carolyn Opio, Jeroen Dijkman, Allessandra Falcucci, and Giuseppe Tempio. *Tackling climate change through livestock: a global assessment of emissions and mitigation opportunities*. Food and Agriculture Organization of the United Nations (FAO), 2013.

[5] Conti, Roberto, Laura Pezzolesi, Rossella Pistocchi, Cristian Torri, Patrizio Massoli, and Daniele Fabbri. "Photobioreactor cultivation and catalytic pyrolysis of the microalga Desmodesmus communis (Chlorophyceae) for hydrocarbons production by HZSM-5 zeolite cracking." *Bioresource technology* 222 (2016): 148-155.

[6] Ong, Hwai Chyuan, Wei-Hsin Chen, Abid Farooq, Yong Yang Gan, Keat Teong Lee, and Veeramuthu Ashokkumar. "Catalytic thermochemical conversion of biomass for biofuel production: A comprehensive review." Renewable and Sustainable Energy Reviews 113 (2019): 109266.

[7] Li, Yue, Yinguang Chen, and Jiang Wu. "Enhancement of methane production in anaerobic digestion process: A review." Applied energy 240 (2019): 120-137.

[8] Zabed, Hossain M., Suely Akter, Junhua Yun, Guoyan Zhang, Faisal N. Awad, Xianghui Qi, and J. N. Sahu. "Recent advances in biological pretreatment of microalgae and lignocellulosic biomass for biofuel production." Renewable and Sustainable Energy Reviews 105 (2019): 105-128.

[9] Yadav, Sudesh Kumar. "Technological advances and applications of hydrolytic enzymes for valorization of lignocellulosic biomass." Bioresource technology 245 (2017): 1727-1739.

[10] National Chicken Council, "National CHICKEN council," 16 5 2020. [Online]. Available: https://www.nationalchickencouncil.org/about-the-industry/statistics/per-capita-consumption-of-poultry-and-livestock-1965-to-estimated-2012-in-pounds/.

[11] United States. Department of Agriculture. Economics, Statistics Service, United States. Foreign Agricultural Service, United States. World Food, Agricultural Outlook, and Situation Board. World Agricultural Supply and Demand Estimates. The Department, 2019.

[12] Sahu, Santi Gopal, N. Chakraborty, and P. Sarkar. "Coal–biomass co-combustion: An overview." *Renewable and Sustainable Energy Reviews* 39 (2014): 575-586.

[13] Lam, Ka Leung, Adetoyese O. Oyedun, and Chi Wai Hui. "Numerical study of mixed-feedstock pyrolysis." In Computer aided chemical engineering, vol. 31, pp. 1311-1315. Elsevier, 2012.

[14] Yang, H., Yan, R., Chen, H., Zheng, C., Lee, D. H., and Liang, D. T., 2006, “InDepth Investigation of Biomass Pyrolysis Based on Three Major Components: Hemicellulose, Cellulose and Lignin,” Energy Fuels, 20(1), pp. 388–393.

[15] Choudhary, Jairam, Surender Singh, and Lata Nain. "Thermotolerant fermenting yeasts for simultaneous saccharification fermentation of lignocellulosic biomass." Electronic Journal of Biotechnology 21 (2016): 82-92.

[16] Rosendahl, Lasse, ed. Biomass combustion science, technology and engineering. Elsevier, 2013.

[17] Hussein, Mohamed Hussein, "Experimental Investigation of Chicken Manure Pyrolysis and Gasification" (2016). Ph.D. Thesis, University of Wisconsin-Milwaukee.

[18] Altman, Arie, and Paul Michael Hasegawa, eds. *Plant biotechnology and agriculture: prospects for the 21st century*. Academic press, 2011.

[19] Bridgwater, A. V. "A survey of thermochemical biomass processing activities." *Biomass* 22, no. 1-4 (1990): 279-292.

[20] Friedman, Henry L. "Kinetics of thermal degradation of char-forming plastics from thermogravimetry. Application to a phenolic plastic." In *Journal of polymer science part C: polymer symposia*, vol. 6, no. 1, pp. 183-195. New York: Wiley Subscription Services, Inc., A Wiley Company, 1964.

[21] Roberts, A. F. "A review of kinetics data for the pyrolysis of wood and related substances." Combustion and flame 14, no. 2 (1970): 261-272.

[22] Neves, Daniel, Henrik Thunman, Arlindo Matos, Luís Tarelho, and Alberto Gómez-Barea. "Characterization and prediction of biomass pyrolysis products." Progress in Energy and Combustion Science 37, no. 5 (2011): 611-630.

[23] Wnetrzak, R., D. J. M. Hayes, Lars Stoumann Jensen, J. J. Leahy, and W. Kwapinski. "Determination of the higher heating value of pig manure." *Waste and Biomass Valorization* 6, no. 3 (2015): 327-333.

[24] Buschow, KH Jürgen, Robert W. Cahn, Merton C. Flemings, Bernhard Ilschner, Edward J. Kramer, and Subhash Mahajan. "Encyclopedia of materials." *Science and technology* 1 (2001): 11.

[25] Khatib, Jamal, ed. *Sustainability of construction materials*. Woodhead Publishing, 2016.

[26] Greenhalf, C. E., D. J. Nowakowski, A. B. Harms, J. O. Titiloye, and A. V. Bridgwater. "A comparative study of straw, perennial grasses and hardwoods in terms of fast pyrolysis products." *Fuel* 108 (2013): 216-230.

[27] Mettler, Matthew S., Alex D. Paulsen, Dionisios G. Vlachos, and Paul J. Dauenhauer. "The chain length effect in pyrolysis: bridging the gap between glucose and cellulose." *Green Chemistry* 14, no. 5 (2012): 1284-1288.

[28] Yang, H., Yan, R., Chen, H., Zheng, C., Lee, D. H., and Liang, D. T., 2006, "InDepth Investigation of Biomass Pyrolysis Based on Three Major Components: Hemicellulose, Cellulose and Lignin," Energy Fuels, 20(1), pp. 388–393.

[29] Wang, Shurong, Gongxin Dai, Haiping Yang, and Zhongyang Luo. "Lignocellulosic biomass pyrolysis mechanism: a state-of-the-art review." *Progress in Energy and Combustion Science* 62 (2017): 33-86.

[30] Chowdhury, Swaptik, Mihir Mishra, and O. M. Suganya. "The incorporation of wood waste ash as a partial cement replacement material for making structural grade concrete: An overview." *Ain Shams Engineering Journal* 6, no. 2 (2015): 429-437.

[31] Zając, Grzegorz, Joanna Szyszlak-Bargłowicz, Wojciech Gołębiowski, and Małgorzata Szczepanik. "Chemical characteristics of biomass ashes." *Energies* 11, no. 11 (2018): 2885.

[32] Dry, Mark E. "Practical and theoretical aspects of the catalytic Fischer-Tropsch process." *Applied Catalysis A: General* 138, no. 2 (1996): 319-344.

[33] Verma, M., S. Godbout, S. K. Brar, O. Solomatnikova, S. P. Lemay, and J. P. Larouche. "Biofuels production from biomass by thermochemical conversion technologies." *International Journal of Chemical Engineering* 2012 (2012).

[34] Heidari, Ava, Eshagh Khaki, Habibollah Younesi, and Hangyong Ray Lu. "Evaluation of fast and slow pyrolysis methods for bio-oil and activated carbon production from eucalyptus wastes using a life cycle assessment approach." Journal of Cleaner Production 241 (2019): 118394.

[35] Balat, M. "Mechanisms of thermochemical biomass conversion processes. Part 1: reactions of pyrolysis." *Energy Sources, Part A* 30, no. 7 (2008): 620-635.

[36] Yang, Haiping, Rong Yan, Hanping Chen, Dong Ho Lee, and Chuguang Zheng. "Characteristics of hemicellulose, cellulose and lignin pyrolysis." *Fuel* 86, no. 12-13 (2007): 1781-1788.

[37] Cho, Joungmo, Jeffrey M. Davis, and George W. Huber. "The intrinsic kinetics and heats of reactions for cellulose pyrolysis and char formation." *ChemSusChem* 3, no. 10 (2010): 1162-1165.

[38] Parthasarathy, Prakash, and K. Sheeba Narayanan. "Hydrogen production from steam gasification of biomass: influence of process parameters on hydrogen yield–a review." *Renewable energy* 66 (2014): 570-579.

[39] Pala, Laxmi Prasad Rao, Qi Wang, Gunther Kolb, and Volker Hessel. "Steam gasification of biomass with subsequent syngas adjustment using shift reaction for syngas production: An Aspen Plus model." *Renewable Energy* 101 (2017): 484-492.

[40] Chaudhari, S. T., S. K. Bej, N. N. Bakhshi, and A. K. Dalai. "Steam gasification of biomass-derived char for the production of carbon monoxide-rich synthesis gas." *Energy & fuels* 15, no. 3 (2001): 736-742.

[41] Reed, Thomas B. *Encyclopedia of biomass thermal conversion: the principles and technology of pyrolysis, gasification & combustion*. Biomass energy foundation Press, 2002.

[42] Cheng, Yongpan, Zhihao Thow, and Chi-Hwa Wang. "Biomass gasification with CO2 in a fluidized bed." *Powder Technology* 296 (2016): 87-101.

[43] Zhou, Jinsong, Qing Chen, Hui Zhao, Xiaowei Cao, Qinfeng Mei, Zhongyang Luo, and Kefa Cen. "Biomass-oxygen gasification in a high-temperature entrained-flow gasifier." *Biotechnology advances* 27, no. 5 (2009): 606-611.

[44] Hussein, M. S., K. G. Burra, R. S. Amano, and A. K. Gupta. "Effect of oxygen addition in steam gasification of chicken manure." *Fuel* 189 (2017): 428-435.

[45] Collot, A-G., Y. Zhuo, D. R. Dugwell, and R. Kandiyoti. "Co-pyrolysis and co-gasification of coal and biomass in bench-scale fixed-bed and fluidised bed reactors." *Fuel* 78, no. 6 (1999): 667-679.

[46] Fan, Yingjie, Yaowu Li, Zhiqiang Wu, Zongyu Sun, and Bolun Yang. "Kinetic analysis on gaseous products during co-pyrolysis of low-rank coal with lignocellulosic biomass model compound: Effect of lignin." *Energy Procedia* 152 (2018): 916-921.

[47] He, Qing, Qinghua Guo, Lu Ding, Juntao Wei, and Guangsuo Yu. "Rapid co-pyrolysis of lignite and biomass blends: Analysis of synergy and gasification reactivity of residue char." *Journal of Analytical and Applied Pyrolysis* 143 (2019): 104688.

[48] Paradela F, Pinto F, Gulyurtlu I, Cabrita I, Lapa N. Study of the co-pyrolysis of biomass and plastic wastes. Clean Technol Environ Policy 2009;11(1): pp. 115-122.

[49] Lam, Ka Leung, Adetoyese O. Oyedun, and Chi Wai Hui. "Numerical study of mixed-feedstock pyrolysis." In Computer aided chemical engineering, vol. 31, pp. 1311-1315. Elsevier, 2012.

[50] Vasile C, Brebu MA. Thermal valorisation of biomass and of synthetic polymer waste. Upgrading of pyrolysis oils. Cellul Chem Technol 2007;40(7): pp.489-512.

[51] Uzoejinwa, B. B., He, X., Wang, S., El-Fatah Abomohra, A., Hu, Y., & Wang, Q. (2018). Co-pyrolysis of biomass and waste plastics as a thermochemical conversion technology for high-grade biofuel production: Recent progress and future directions elsewhere worldwide. Energy Conversion and Management, vol. 163, pp. 468–492. doi:10.1016/j.enconman.2018.02.004

[52] K. . Dang et al., "Catalytic Pyrolysis of Rice Husk via Semi-Batch Reactor Using L9 Taguchi Orthogonal Array", Advanced Materials Research, Vol. 787, pp. 184-189, 2013

[53] Ahiduzzaman, Md, and AKM Sadrul Islam. "Thermo-gravimetric and kinetic analysis of different varieties of rice husk." Procedia Engineering 105 (2015): pp.646-651.

[54] Hossain, M. S., Islam, M. R., Rahman, M. S., Kader, M. A., & Haniu, H. (2017). Biofuel from Co-pyrolysis of Solid Tire Waste and Rice Husk. In Energy Procedia (Vol. 110, pp. 453–458). Elsevier Ltd. https://doi.org/10.1016/j.egypro.2017.03.168

[55] Costa, P., Pinto, F., Miranda, M., André, R., & Rodrigues, M. (2014). Study of the experimental conditions of the co-pyrolysis of rice husk and plastic wastes. Chemical Engineering Transactions, 39 (Special Issue), pp. 1639–1644. https://doi.org/10.3303/CET1439274

[56] GUO, Xiu-juan, Shu-rong WANG, Kai-ge WANG, L. I. U. Qian, and Zhong-yang LUO. "Influence of extractives on mechanism of biomass pyrolysis." Journal of fuel Chemistry and Technology 38, no. 1 (2010): pp.42-46.

[57] Mallick, Debarshi, Maneesh Kumar Poddar, Pinakeswar Mahanta, and Vijayanand S. Moholkar. "Discernment of synergism in pyrolysis of biomass blends using thermogravimetric analysis." Bioresource technology 261 (2018): 294-305.

[58] Dayananda, B. S., S. H. Manjunath, K. B. Girish, and L. K. Sreepathi. "An experimental approach on Gasification of the chicken litter with Rice husk." International Journal of Innovative Research in Science, Engineering and Technology 2, no. 7 (2013), pp. 2837-2842

[59] Alauddin, Zainal Alimuddin Bin Zainal, Pooya Lahijani, Maedeh Mohammadi, and Abdul Rahman Mohamed. "Gasification of lignocellulosic biomass in fluidized beds for renewable energy development: A review." *Renewable and Sustainable Energy Reviews* 14, no. 9 (2010): 2852-2862.

[60] Dayananda, B. S., and L. K. Sreepathi. "Design and analysis of fluidized bed gasifier for chicken litter along with agro wastes." *Int Res J Environ Sci* 1, no. 3 (2012): 11-6.

[61] Wagenaar, B. M., W. Prins, and W. P. M. Van Swaaij. "Pyrolysis of biomass in the rotating cone reactor: modelling and experimental justification." *Chemical Engineering Science* 49, no. 24 (1994): 5109-5126.

[62] Tamminen, Jarmo. "Thermal analysis for investigation of solidification mechanisms in metals and alloys." PhD diss., University of Stockholm, 1988.

[63] White, John E., W. James Catallo, and Benjamin L. Legendre. "Biomass pyrolysis kinetics: a comparative critical review with relevant agricultural residue case studies." Journal of analytical and applied pyrolysis 91, no. 1 (2011): pp.1-33.

[64] Vyazovkin, Sergey, and Charles A. Wight. "Model-free and model-fitting approaches to kinetic analysis of isothermal and nonisothermal data." *Thermochimica acta* 340 (1999): 53-68.

[65] Neuhaus, Gerd W., and Wilhelm F. Maier. "A general integral method for the determination of empirical reaction rates and parameters." *Chemical Engineering & Technology: Industrial Chemistry-Plant Equipment-Process Engineering-Biotechnology* 19, no. 3 (1996): 249-262.

[66] Luo, Laipeng, Xiaojuan Guo, Zhen Zhang, Meiyun Chai, Md Maksudur Rahman, Xingguang Zhang, and Junmeng Cai. "Insight into Pyrolysis Kinetics of Lignocellulosic Biomass: Isoconversional Kinetic Analysis by the Modified Friedman Method." *Energy & Fuels* 34, no. 4 (2020): 4874-4881.

[67] Wang, Jinwu, Marie-Pierre G. Laborie, and Michael P. Wolcott. "Comparison of model-free kinetic methods for modeling the cure kinetics of commercial phenol–formaldehyde resins." *Thermochimica Acta* 439, no. 1-2 (2005): 68-73.

[68] Gaur, Siddhartha, and Thomas B. Reed. An atlas of thermal data for biomass and other fuels. No. NREL/TP-433-7965. National Renewable Energy Lab., Golden, CO (United States), 1995.

[69] Kim, Seung-Soo, and Foster A. Agblevor. "Pyrolysis characteristics and kinetics of chicken litter." *Waste Management* 27, no. 1 (2007): 135-140.

[70] Lim, Aaron Chee Ren, Bridgid Lai Fui Chin, Zeinab Abbas Jawad, and Kiew Ling Hii. "Kinetic analysis of rice husk pyrolysis using Kissinger-Akahira-Sunose (KAS) method." *Procedia engineering* 148 (2016): 1247-1251.

[71] Sobek, Szymon, and Sebastian Werle. "Kinetic modelling of waste wood devolatilization during pyrolysis based on thermogravimetric data and solar pyrolysis reactor performance." Fuel 261 (2020): 116459

[72] Selim, Osama M., Mohamed S. Hussein, and Ryoichi S. Amano. "Effect of Heating Rate on Chemical Kinetics of Chicken Manure With Different Gas Agents."

[73] Tsai, W. T., M. K. Lee, and Y. M. Chang. "Fast pyrolysis of rice husk: Product yields and compositions." *Bioresource technology* 98, no. 1 (2007): 22-28.

[74] Funazukuri, Toshitaka, Robert R. Hudgins, and Peter L. Silveston. "Correlation of volatile products from fast cellulose pyrolysis." *Industrial & Engineering Chemistry Process Design and Development* 25, no. 1 (1986): 172-181.

[75] Rieger, J. "The glass transition temperature of polystyrene." *Journal of thermal analysis* 46, no. 3-4 (1996): 965-972.

[76] Glass, Herbert David. "Investigation of rank in coal by differential thermal analysis." *Economic Geology* 49, no. 3 (1954): 294-309.

[77] Instruments, Shimadzu Scientific. “DTG-60/60 Simultaneous Thermogravimetry/Differential Thermal Analyzers.” Differential Thermal Thermogravimetry Analyzer | Shimadzu DTG-60/60, March 30, 2020. https://www.ssi.shimadzu.com/products/thermal-analysis/dtg-60.html.

[78] Phyllis.nl. 2000. *Phyllis2 - ECN Phyllis Classification*. [online] Available at: <https://phyllis.nl/Browse/Standard/ECN-Phyllis#chicken%20manure> [Accessed 1 May 2020].

[79] Ummah, H., D. A. Suriamihardja, M. Selintung, and A. W. Wahab. "Analysis of the chemical composition of rice husk used as absorber plates sea water into clean water." ARPN Journal of Engineering and Applied Sciences 10, no. 14 (2015): pp. 6046-6050.

[80] Kamruzzaman, M., and AKM Sadrul Islam. "physical and thermochemical properties of rice husk in Bangladesh." International Journal of BioResearch 6 (2011): pp.45-49.

[81]Tańczuk, Mariusz, Robert Junga, Alicja Kolasa-Więcek, and Patrycja Niemiec. "Assessment of the Energy Potential of Chicken Manure in Poland." Energies 12, no. 7 (2019): pp.1244-1262

[82] Chen, Chao, Siqian Zhang, Kyung Ho Row, and Wha-Seung Ahn. "Amine–silica composites for CO2 capture: A short review." Journal of energy chemistry 26, no. 5 (2017): 868-880.

[83] Ciferno, Jared. “ Syngas Optimized for Intended Products.” netl.doe.gov. National Energy Technology Laboratory, 2002. https://www.netl.doe.gov/research/coal/energy-systems/gasification/gasifipedia/syngas-optimization.

[84] Cao, Yan, Zhengyang Gao, Jing Jin, Hongchang Zhou, Marten Cohron, Houying Zhao, Hongying Liu, and Weiping Pan. "Synthesis gas production with an adjustable H2/CO ratio

through the coal gasification process: effects of coal ranks and methane addition." Energy & fuels 22, no. 3 (2008): 1720-1730.

[85] Boateng, A. A., Mullen, C. A., Osgood-Jacobs, L., Carlson, P., and Macken, N., 2012, “Mass Balance, Energy, and Exergy Analysis of Bio-Oil Production by Fast Pyrolysis,” ASME J. Energy Resource. Technol., 134(4), p. 042001-1.

103(4), pp. 344–351.

[86] Lima, Isabel M., Akwasi A. Boateng, and K. Thomas Klasson. "Pyrolysis of broiler manure: Char and product gas characterization." *Industrial & engineering chemistry research* 48, no. 3 (2009): 1292-1297.

[87] Loy, Adrian Chun Minh, Suzana Yusup, Bridgid Lai Fui Chin, Darren Kin Wai Gan, Muhammad Shahbaz, Menandro N. Acda, Pornkamol Unrean, and Elisabeth Rianawati. "Comparative study of in-situ catalytic pyrolysis of rice husk for syngas production: kinetics modelling and product gas analysis." *Journal of Cleaner Production* 197 (2018): 1231-1243.

[88] McAllister, Sara, Jyh-Yuan Chen, and A. Carlos Fernandez-Pello. *Fundamentals of combustion processes*. Vol. 302. New York: Springer, 2011.

Appendix A: DTA charts for different heating rates

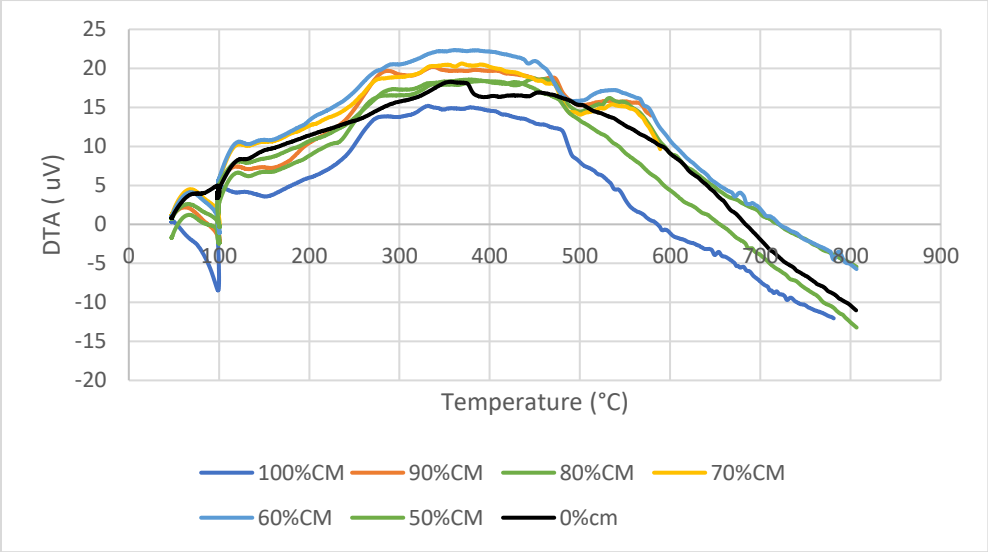

Figure 36 DTA for different blends at 10°C/min

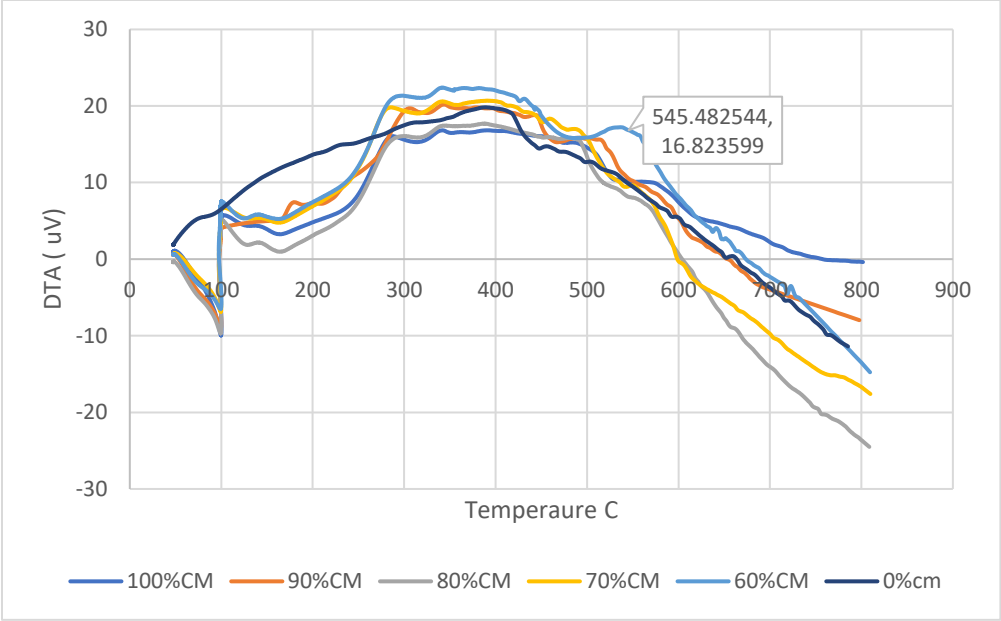

Figure 37 DTA for different blends at 15°C/min

Appendix B: Semi-empirical model program script

```
Ti=350;
%Chemical composition of chicken manure
yt1=0.9*35;
ycf1 =34.51/100*yt1;
yhf1=4.79/100*yt1;
yof1=26.31/100*yt1;
ynf1=3.42/100*yt1;
%Chemical composition of rice husk
yt2=35*0.89;
ycf2=27.92/100*yt2;
yhf2=4.23/100*yt2;
yof2=37.86/100*yt2;
ynf2=0.49/100*yt2;
%mixing ratio f
fi=0;
t=0;
beta=50;
n=floor((1000-Ti)/beta);
A=zeros (7,7);
B=zeros(7,1);
LHVg=-6.23+2.47*10^-2*Ti;%First iteration
LHVgas=zeros (n,1);
Tramp=zeros (n,1);
Ytar=zeros(n,1);
```

```
Ygas=zeros(n,1);
totaloles=0;

for fi=0:0.1:1
T=Ti;
f=fi

yt=(f)*yt1+(1-f)*yt2;
mcf=(f)*ycf1+(1-f)*ycf2;
mof=(f)*yof1+(1-f)*yof2;
mhf=(f)*yhf1+(1-f)*yhf2;
mnf=(f)*ynf1+(1-f)*ynf2;
ych=f*(-0.0003*T+0.4163)+(1-f)*(-0.0002*T+0.3757);%empirical data for biomass
pyrolysis free ashes (-0.20) from 400 to 1000

    while T<1000


        %Matrix A construction
        A(1,1)=(1.05+1.9*10^(-4)*T)*mcf;%'Yctar'
        A(1,2)=24/28;%Yc/c2h4
        A(1,3)=12/16;%Yc/ch4
        A(1,4)=12/28;%yc/CO
        A(1,5)=12/44;%yc/co2
        %A(1,6),A(1,7)=0;
        A(2,1)=(0.92-2.2*10^(-4)*T)*mof; %Yotar
        A(2,4)=16/28;
        A(2,5)=32/44;
        A(2,6)=16/18;%yoh2o

        A(3,1)=(0.93+3.8*10^(-4)*T)*mhf;%'Yhtar'
        A(3,2)=4/28; %yh,c2h4
        A(3,3)=4/16;%yh,ch4
        A(3,6)=2/18;
        A(3,7)=2/2;
        A(4,4)=1;
        A(4,7)=-13.407;

        A(5,3)=-1;
        A(5,4)=0.146;
        A(6,1)= LHVg; %Approximate LHV of gas
        A(6,2)=47.1;%LHV C2H4 (majority of heavy cxhn in chicken experiments)
        A(6,3)=50;%LHV of methane (MJ/kg)
        A(6,4)=10.1;%LHV of CO
        A(6,5)=0;
        A(6,6)=A(6,1);
        A(6,7)=120;%LHV of H2
        A(7,7)=1;
        mcch=0.93-0.92*exp(-0.42*10^(-2)*T);
        moch=0.07-0.85*exp(-0.48*10^(-2)*T);
        mhch=-0.0041+0.10*exp(-0.24*10^(-2)*T);
        Sumyfj=mcf+mhf+mof;
        sumyfch=mcch+moch+mhch;
        %Matrix B construction
        B(1,1)=mcf-mcch*ych;
```

```
        B(2,1)=mof-moch*ych;
        B(3,1)=mhf-mhch*ych;
        B(4,1)=0.0688;
        B(5,1)=2.18*10^-4;
        B(6,1)=(Sumyfj-ych*(sumyfch))*LHVg;
        B(7,1)=0.0038*exp(0.0052*T);
        X={'ytar','yc2h4','ych4','yco','yco2','yh20','yh2'};
        X=A\B;
        t=t+1;
        T=T+beta;
        Tramp(t)=T;
       %Results

        Ygas(t)=(X(7)+X(5)+X(4)+X(3)+X(2))/yt;
        totalmoles= (X(7)/2+X(5)/44+X(4)/28+X(3)/16+X(2)/28);
        YCO2=(X(5)/44)/totalmoles;
        YCO=(X(4)/28)/totalmoles;
        YCH4=(X(3)/16)/totalmoles;
        YCXHM=(X(2)/28)/totalmoles;
        YH2=(X(7)/2)/totalmoles;
        E(t)=(120*X(7)+10.1*X(4)+50*X(3)+47.1*X(2));
        LHVgas(t)=E(t)/(sum(X));
        Ytar(t)=X(1)/yt;
    end

Energy=E;
Tramp;
LHVgas;

t=0;
end

plot(Tramp,LHVgas)
xlabel('Temperature (°C)')
ylabel('LHV kJ/kg')
hold on
yyaxis right;
plot(Tramp,Ygas)
plot (Tramp,Ytar)
hold off
```